



Article

Biogeography-Based Teaching Learning-Based Optimization Algorithm for Identifying One-Diode, Two-Diode and Three-Diode Models of Photovoltaic Cell and Module

Nawal Rai ^{1,*}, Amel Abbadi ², Fethia Hamidia ², Nadia Douifi ¹, Bdereddin Abdul Samad ^{3,*} 
and Khalid Yahya ⁴ 

¹ Advanced Electronic Systems Laboratory (AESL), Electrical Engineering Department, Faculty of Technology, Dr. Yahia Fares University, Medea 26000, Algeria; douifi.nadia@univ-medea.dz

² Electrical Engineering and Automatic Laboratory (EEAL), Electrical Engineering Department, Faculty of Technology, Dr. Yahia Fares University, Medea 26000, Algeria; abbadi.amel@univ-medea.dz (A.A.); hamidia.fethia@univ-medea.dz (F.H.)

³ School of Engineering, Cardiff University, Cardiff CF24 3AA, UK

⁴ Department of Electrical and Electronics Engineering, Nisantasi University, Istanbul 34467, Turkey; khalid.yahya@nisantasi.edu.tr

* Correspondence: rai.nawal@univ-medea.dz (N.R.); abdulsamadbf@cardiff.ac.uk (B.A.S.)

Abstract: This article handles the challenging problem of identifying the unknown parameters of solar cell three models on one hand and of photovoltaic module three models on the other hand. This challenge serves as the basis for fault detection, control, and modelling of PV systems. An accurate model of PV is essential for the simulation research of PV systems, where it has a significant role in the dynamic study of these systems. The mathematical models of the PV cell and module have nonlinear I-V and P-V characteristics with many undefined parameters. In this paper, this identification problem is solved as an optimization problem based on metaheuristic optimization algorithms. These algorithms use root mean square error (RMSE) between the calculated and the measured current as an objective function. A new metaheuristic amalgamation algorithm, namely biogeography-based teaching learning-based optimization (BB-TLBO) is proposed. This algorithm is a hybridization of two algorithms, the first one is called BBO (biogeography-based optimization) and the second is TLBO (teaching learning-based optimization). The BB-TLBO is proposed to identify the unknown parameters of one, two and three-diode models of the RTC France silicon solar cell and of the commercial photovoltaic solar module monocrystalline STM6-40/36, taking into account the performance indices: high precision, more reliability, short execution time and high convergence speed. This identification is carried out using experimental data from the RTC France silicon solar cell and the STM6-40/36 photovoltaic module. The efficiency of BB-TLBO is checked by comparing its identification results with its own single algorithm BBO, TLBO and newly introduced hybrid algorithms such as DOLADE, LAPSO and others. The results reveal that the suggested approach surpasses all compared algorithms in terms of RMSE (RMSE min, RMSE mean and RMSE max), standard deviation of RMSE values (STD), CPU (execution time), and convergence speed.

Keywords: photovoltaic cell and module; biogeography-based optimization; teaching learning-based optimization algorithm; identifying the unknown parameters; double-diode model; three-diode model

MSC: 68T20; 90C26



Citation: Rai, N.; Abbadi, A.; Hamidia, F.; Douifi, N.; Abdul Samad, B.; Yahya, K. Biogeography-Based Teaching Learning-Based Optimization Algorithm for Identifying One-Diode, Two-Diode and Three-Diode Models of Photovoltaic Cell and Module. *Mathematics* **2023**, *11*, 1861. <https://doi.org/10.3390/math11081861>

Academic Editors: Adrian Deaconu, Petru Adrian Cotfas, Daniel Tudor Cotfas and Alessandro Niccolai

Received: 15 March 2023

Revised: 9 April 2023

Accepted: 10 April 2023

Published: 14 April 2023



Copyright: © 2023 by the authors. Licensee MDPI, Basel, Switzerland. This article is an open access article distributed under the terms and conditions of the Creative Commons Attribution (CC BY) license (<https://creativecommons.org/licenses/by/4.0/>).

1. Introduction

Air and environmental pollution, rising costs, and possible depletion of fossil fuels are disadvantages of generating electricity from fossil fuels [1]. To minimize these disadvantages, a new energy strategy has been developed using new clean energy technologies such as solar, wind, nuclear, tidal, etc. [2,3]. Renewable energy power production has

been significantly increasing worldwide [4]. Among all the sources of renewable energies, solar energy holds the most promise. Inherent characteristics of semiconductors are used by photovoltaic systems to convert sun energy to electrical energy which represents a direct way of converting [5]. However, there are still significant obstacles to the practical implementation of solar energy, such as low photoelectric conversion efficiency as well as a lack of precision in the modelling of PV cells [6]. Furthermore, more precise PV modelling can lead to the development of more advanced and efficient solar technologies, such as new types of solar cells and modules. These technologies can be optimized and tested through accurate modelling, allowing for rapid progress in the field of solar energy. Additionally, more accurate modelling can improve the predictability of solar energy production, making it easier to integrate solar energy into the existing power grid and increasing the stability of the grid as a whole. This can also contribute to the overall reduction of greenhouse gas emissions and the transition toward a cleaner and more sustainable energy system.

Accurate modelling of photovoltaic cells is very important to study the performance of photovoltaic systems [7]. One-diode model (1DM) [8], improved one-diode model (I1DM) [9], two-diode model (2DM) [10], modified two-diode model (M2DM) [10] and three-diode model (3DM) [11,12], are some of the PV models that have been developed.

The most frequently used approaches in the literature to determine the parameters of PV models are deterministic methods and flexible computational techniques.

The deterministic methods involve analytical and computational methods. The analytical method makes use of a number of locations along the current–voltage curve (I-V); therefore, their effectiveness largely depends on the points that are chosen [13]. In contrast, the computational method implements curve fit. This last procedure necessitates numerous calculations. The appropriate choice of the fitting method will determine its correctness. The large number of parameters increases the algorithm's complexity and limits its ability to estimate accurate values [14–16].

According to the literature, some researchers use flexible computational methods to determine the parameters of PV models such as Fuzzy Logic reasoning (FL) [17], Artificial Neural Network (ANN) [18,19], Adaptive Neuro-Fuzzy Inference System (ANFIS) [20] . . . etc. Although these methods produced decent fitting results, they required very high computational capacity with skilled personnel to train the datasets [21].

To overcome the drawbacks of the previous techniques, another approach has been developed, that of metaheuristic methods. The latter has been the subject of several studies in the literature. These techniques are more suitable for estimating PV parameters and they are efficient with multimodal functions. They transform the PV cell parameter extraction problem into an optimization problem. Its objective is to minimize the fitness metric function by a metaheuristic optimization algorithm [1,22].

In the last few decades, metaheuristic algorithms have greatly increased in popularity for solving challenging multi-objective optimization problems in a variety of engineering disciplines. Its importance for the PV parameter identification problem was prompted by its enormous capacity for identifying potential solutions. The Genetic Algorithm (GA) was the first metaheuristic algorithm to evolve, followed by Differential Evolution (DE) and Particle Swarm Optimization. (PSO) [23].

GA is a population-based algorithm inspired by biology that mimics the “survival of the fittest” phenomenon. It has three main steps: selection, crossover and mutation. In the problem of PV identification parameters, GA is a better utilization of search space due to mutation and crossover operations and it is good in exploration but it suffers from a high computational burden and is poor in exploitation [23]. To reduce the computational burden of GA, a hybrid strategy (GA + NR) has been proposed in [24]. In this strategy, GA was used to extract three parameters, R_s , R_{sh} and n whereas I_{ph} and I_s were extracted analytically using Newton Raphson (NR) method. According to the findings, the NR technique converges quickly when the number of unknowns is small, Low computational burden and accuracy depends on the parameters that GA has optimized. Another version of GA which is hybridization between GA and the interior point method is proposed in [25].

This algorithm GA +IP was used to identify the parameters of 1DM taking into account the standard and nominal operating cell temperature (NOCT) conditions of a PV. The results of GA + IP indicate that this algorithm is accurate in real-time operating conditions, multi-objective-based optimization and slow convergence. In addition to the two previous versions of GA a new variant is developed and presented in [26]. This algorithm is Genetic Algorithm with Convex Combination Crossover (GACCC), it is proposed to identify the one-diode model, the two-diode model and the PV module. GACCC is accomplished through the inclusion of a new crossover operation to maintain a good balance between intensifying the best solutions and diversifying the search space. The results show a high accuracy and efficiency of GACCC in identifying parameters. Moreover, there are other variants and modifications of GA that have not been implemented, such as the Stud-Genetic Algorithm (SGA) [27], which might have a high impact on PV identification parameters.

Differential evolution is a heuristic, population-based algorithm originally proposed by Storn and Price in 1997. DE has mainly four stages: initialization, mutation, crossover, and selection. In the problem of identifying parameters, DE lacks the ability to attain a good optimization effect and does not accurately identify the model parameters, resulting in a bias in describing the internal behaviour of photovoltaic systems due to a weak global optimization capability, which will easily converge to the local optimum. Furthermore, it is overly dependent on the initial value of the mutation and crossover factor [23]. To overcome the above shortcoming, several variants of DE have been introduced. In [27], authors have introduced an improved DE (DVADE) to identify the parameters of 1DM and 2DM of the solar cell and PV module. This algorithm is based on reusing previous individual vectors and an adaptive mutation strategy. In this algorithm DVADE, to enhance the effectiveness of differential evolution, the successful difference vectors from earlier generations are introduced to create the offspring in the following generations. The results demonstrate the accuracy, reliability and convergence speed of DVADE. Another variant of DE used to identify PV parameters has been proposed in [28], this proposed algorithm is based on an adaptation of the DE technique (DET). The adaptation is achieved through crossover and mutation factors. DVADE is compared to GA, chaos particle swarm optimization (CPSO), harmony search algorithm (HSA), and artificial bee swarm optimization (ABSO). The outcome shows that it is an optimal method which suits the parameter extraction of solar cells and modules. Recently, authors proposed an adaptive differential evolution (ADE) with the dynamic opposite learning strategy (DOL), called DOLADE. The opposite learning approach in DOLADE increases both the elite population and the population of underperformers, enhancing the particles' capacity for exploration. The outcomes show that DOLADE brings superior competition in terms of accuracy, dependability, and computational efficiency when it comes to extracting the best parameters for each PV cell model [29].

Biogeography-based optimization (BBO) was introduced by Dan Simon in 2008 [30]. The BBO was applied to solve many optimization problems, and it proves its efficiency in finding optimal solutions. This is due to its good exploration feature for the current population. Nevertheless, BBO suffers from some drawbacks such as poorness in exploitation features, negligence of the best individuals over generations, and generation of infeasible solutions [30,31]. To overcome the above-mentioned disadvantages, various hybrids and variants of BBO have been proposed. In [32] biogeography-based heterogeneous cuckoo search (BHCS) algorithm has been proposed. This algorithm is a hybrid of two metaheuristic algorithms namely: BBO and Cuckoo Search (CS). BHCS is used to identify 1DM and 2DM of solar cell and two PV modules. The results show that BHCS is accurate and reliable compared to BBO and CS and other metaheuristic algorithms. In addition to BHCS, another version of BBO, the BBO-M algorithm has been proposed in [31]. BBO-M is used to identify two types of cells: solar cells and fuel cells. In this algorithm, the mutation step of DE and the chaos theory are integrated into the BBO structure for enhancing the global searching capability of the algorithm. The results show that BBO-M has fast convergence speed and it can produce solutions of high quality in both types.

The teaching learning-based optimization (TLBO) technique was introduced by RV Rao et al. in 2012 [2]. TLBO algorithm mimics the school strategy in learning. TLBO comprises two fundamental stages, the teacher phase, and the learner phase. In the first phase, the best individual is selected to be a teacher, and in the second phase, learners receive knowledge from each other. In the PV identification problem, TLBO is simple to understand, easy to implement, and good at exploitation however TLBO has some shortcomings like convergence speed, it may require a large number of iterations to converge to the best solution, lack of diversity, it may suffer from a lack diversity in the population, which can limit its exploration capabilities and prevent it from escaping from local optima [23]. To overcome these limitations, various modifications of TLBO such as improving and hybridization with other algorithms have been proposed. In [3], the authors develop a new optimization method called oppositional teaching learning-based optimization (GOTLBO) to identify the parameters of both 1DM and 2DM. The initialization step and generation jumping of this algorithm are taken from generalized opposition-based learning (GOBL) and integrated into the original TLBO. This algorithm was compared with four evolutionary algorithms: jDE, CLPSO, TLBO, and OTLBO. The results show that GOTLBO is very competitive compared to other algorithms. Another variant of TLBO has been proposed in [2]. The authors proposed a hybrid adaptive teaching-learning-based optimization with differential evolution (ATLDE) reliably identify the unknown parameters of both 1DM and 2DM of solar cell and 1DM of two PV modules. In order to verify the performance of ATLDE, it is compared with TLBO, DE and other state-of-the-art metaheuristic algorithms. The results demonstrate that ATLDE can obtain more accurate or similar values, and consume fewer computing resources. In addition to all the algorithms cited above, there are many metaheuristic algorithms used to identify PV parameters, such as the Social Network Optimization (SNO) algorithm [33], the Firefly Algorithm (FA) [34], the Fireworks Algorithm (Fwa) [35], Modified Bald Eagle Search Optimization Algorithm [36], Supply Demand algorithm (SD) [37] and Northern Goshawk Optimization algorithm [38].

In this paper, a new variant of the TLBO algorithm is developed to determine the parameters of PV models that achieve better results in terms of accuracy, robustness and conversion speed. This algorithm is a biogeography-based-teaching-learning-based optimization (BB-TLBO) algorithm which is a hybridization of BBO with TLBO. This algorithm aims to combine the benefits of both TLBO and BBO to strike a balance between exploration and exploitation for a good search process. BB-TLBO not only overcomes the respective limitations of BBO and TLBO but also demonstrates improved performance in determining the parameters of PV models, setting a new benchmark for optimization methods in the field. The BB-TLBO is used for the identification of the PV parameters of the RTC France silicon solar cell and the estimation of the PV parameters of the commercial solar PV module: the monocrystalline STM6-40/36 module.

In this identification process, the one-diode model (1DM), two-diode model (2DM), and three-diode model (3DM) were considered. It is worth mentioning that there are only a few research papers that had done parameter identification of 3DM of PV cell and module, therefore authors are motivated to study this model because it is more accurate compared to the other two models (1DM and 2DM).

In 1DM there are five parameters identified as photocurrent I_{ph} , current saturation I_{s1} , series resistance R_s , shunt resistance R_{sh} and ideality factor n_1 . For 2DM, in addition to the first five parameters, two more parameters are introduced: ideality factor n_2 and the saturation current I_{s2} of the second diode. For 3DM, in addition to the previous seven parameters, two more parameters are added: saturation current I_{s3} and the ideality factor n_3 of the third diode.

The BB-TLBO algorithm is first compared to BBO and TLBO and the results confirm that BB-TLBO outperformed both individual algorithms (BBO and TLBO). Then, the results of BB-TLBO are compared with the reported results of other algorithms recently introduced in the literature. The comparison results demonstrate that BB-TLBO is more accurate, and reliable, with high convergence speed and a short time of execution.

The novelty and main contribution of this paper are as follows:

- The biogeography-based teaching learning optimization (BB-TLBO) algorithm is proposed to efficiently identify PV model parameters.
- The identification is based on three models: 1DM, 2DM and 3DM of two cases, namely the RTC France silicon solar cell and the monocrystalline STM6-40/36 module.
- In BB-TLBO, to balance between the exploitation and exploration, the initialization process and migration step of BBO are integrated into the original form of TLBO before the teaching phase and learner phase and after these steps, an elitism process which is taken from BBO is added at the end.
- The results are compared with BBO, TLBO algorithms, and other reported state-of-the-art algorithms.
- The results show that the BB-TLBO algorithm demonstrates improved performance in determining the parameters of PV models, setting a new benchmark for optimization methods in the field.

The rest of this article is structured as follows: Solar PV cell models with their objective functions are discussed in Section 2. Section 3 presents the description of BB-TLBO pseudocode and its flowchart. The presentation of the experimental results and the discussion of the comparative study are presented in Section 4. Finally, the conclusion is treated in Section 5.

2. Equivalent Circuit for PV Cell/Module Models and Problem Formulation

The three most common models used to simulate photovoltaic cells or modules are presented in this section. These models are one-diode model (1DM), two-diode model (2DM) and three-diode model (3DM). They are discussed in detail below.

2.1. PV Cell Models

2.1.1. One-Diode Model (1DM)

The 1DM is composed of a photo-generated current represented as a current source in parallel with a diode and a so-called shunt resistance R_{sh} , all in series with a resistance R_s as shown in Figure 1. The current output can be formulated as:

$$I_L = I_{ph} - I_{d1} - I_{sh} \tag{1}$$

where: the photo-generated-current, the diode-current and the shunt-resistance-current are denoted by I_{ph} , I_{d1} and I_{sh} respectively. The I_{d1} can be calculated according to Shockley as follows:

$$I_{d1} = I_{s1} \left(\exp \left(\frac{V_L + I_L R_s}{n_1 V_t} \right) - 1 \right) \tag{2}$$

I_{s1} : Diode reserve saturation current, V_L : Output voltage, n_1 : Diode ideality constant and V_t represents junction thermal voltage, it is formulated as:

$$V_t = \frac{KT}{q} \tag{3}$$

where: $K = 1.3806503 \times 10^{-23}$ J/K stands for the constant of the Boltzmann, $q = 1.60217646 \times 10^{-19}$ C stands for electron charge and T stands for junction temperature in Kelvin. The parallel resistance current I_{sh} is calculated as:

$$I_{sh} = \left(\frac{(V_L + I_L R_s)}{R_{sh}} \right) \tag{4}$$

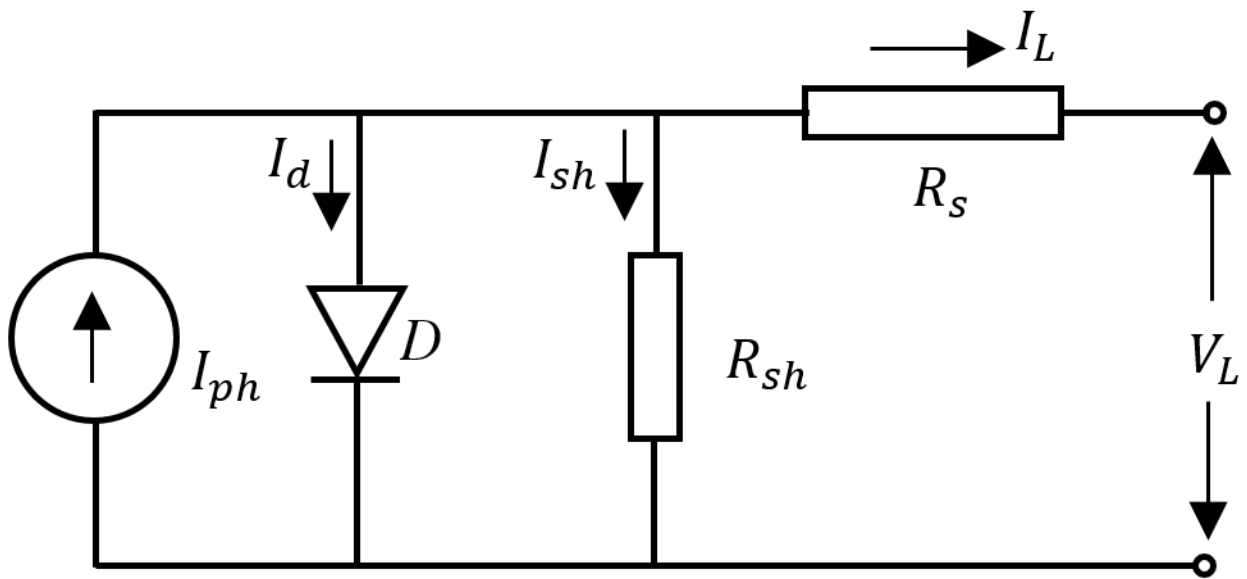


Figure 1. Equivalent circuit of 1DM solar cell.

After replacing Equations (2) and (4) in Equation (1), the output current of the one-diode model is:

$$I_L = I_{ph} - I_{s1} \left(\exp \left(\frac{V_L + I_L R_s}{n_1 V_t} \right) - 1 \right) - \left(\frac{V_L + I_L R_s}{R_{sh}} \right) \tag{5}$$

2.1.2. Two-Diode Model (2DM)

As illustrated in Figure 2, the 2DM consists of two diodes (D1 replicates minority carrier diffusion in the depletion layer, and D2 depicts carrier recombination in the junction’s space charge area) linked in parallel with the current source, and a shunt resistance R_{sh} . this combination is linked in series with a resistance R_s [39].

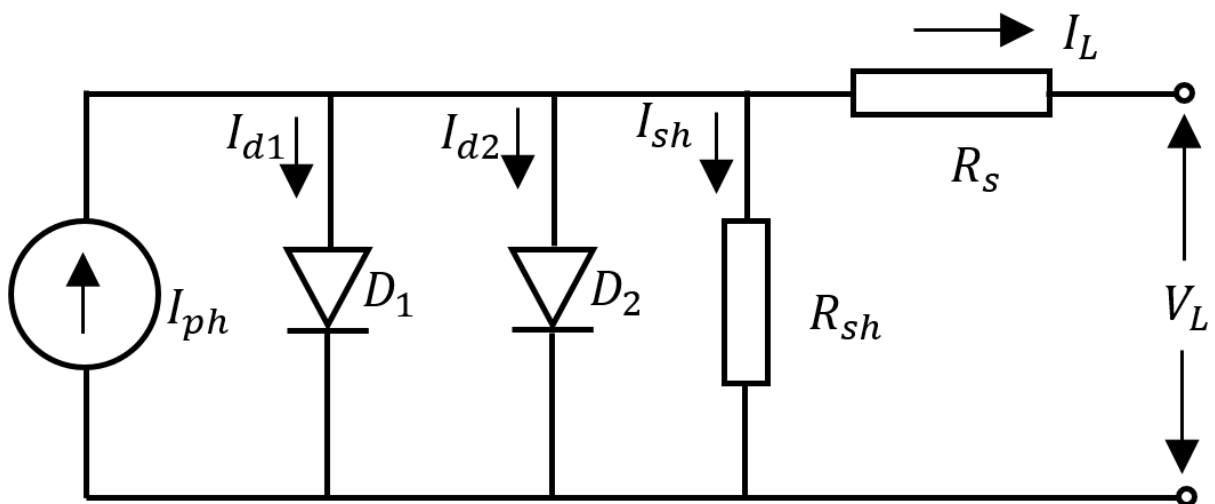


Figure 2. Equivalent circuit of 2DM solar cell.

I-V relationship can be stated by using Kirchhoff’s current law with the Shockley diode equation as follows:

$$I_L = I_{ph} - I_{s1} \left(\exp \left(\frac{V_L + I_L R_s}{n_1 V_t} \right) - 1 \right) - I_{s2} \left(\exp \left(\frac{V_L + I_L R_s}{n_2 V_t} \right) - 1 \right) - \left(\frac{V_L + I_L R_s}{R_{sh}} \right) \tag{6}$$

2.1.3. Three-Diode Model (3DM)

In 3DM, the third diode is introduced in parallel with 2DM as shown in Figure 3 to simulate recombination in the defect region, grain borders and large leakage current as exposed. The I-V relationship can be expressed by using Kirchhoff’s current law and Shockley diode equation as follows [40]:

$$I_L = I_{ph} - I_{s1} \left(\exp\left(\frac{V_L + I_L R_s}{n_1 V_t}\right) - 1 \right) - I_{s2} \left(\exp\left(\frac{V_L + I_L R_s}{n_2 V_t}\right) - 1 \right) - I_{s3} \left(\exp\left(\frac{V_L + I_L R_s}{n_3 V_t}\right) - 1 \right) - \left(\frac{V_L + I_L R_s}{R_{sh}} \right) \quad (7)$$

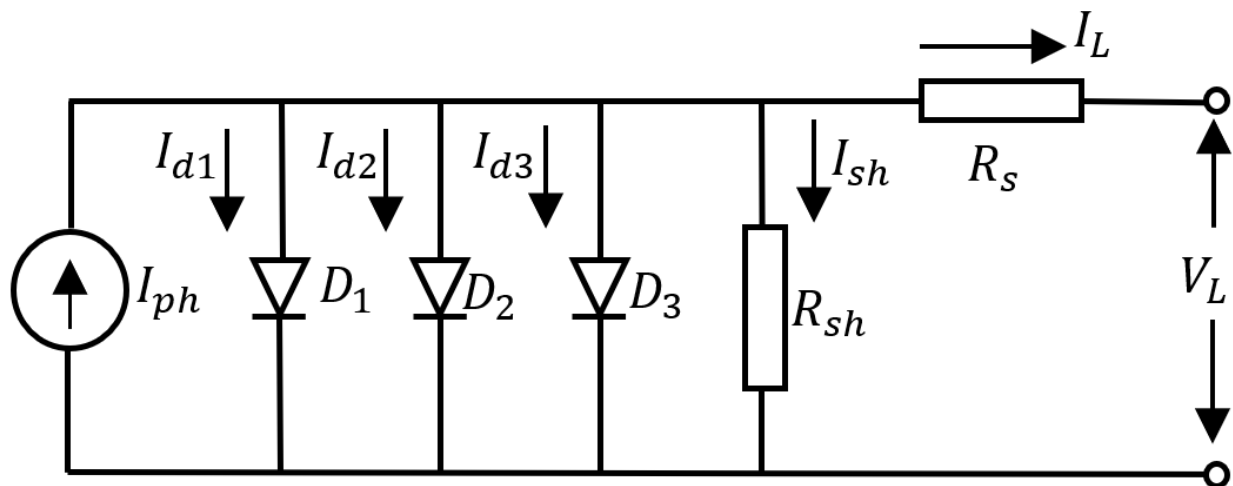


Figure 3. Equivalent circuit of 3DM solar cell.

2.2. PV Module Models

The equivalent circuit of the PV module is exposed in Figure 4. Equations (8)–(10), provide output current equations for 1DM, 2DM, and 3DM, respectively.

$$I_L = I_{ph} N_p - I_{s1} N_p \left[\exp\left(\frac{q((V_L / N_s) + N_s R_s (I_L / N_p))}{n_1 V_t N_s}\right) - 1 \right] - \left(\frac{((V_L / N_s) + N_s R_s (I_L / N_p))}{R_{sh} (N_s / N_p)} \right) \quad (8)$$

$$I_L = I_{ph} N_p - I_{s1} N_p \left[\exp\left(\frac{q((V_L / N_s) + N_s R_s (I_L / N_p))}{n_1 V_t N_s}\right) - 1 \right] - I_{s2} N_p \left[\exp\left(\frac{q((V_L / N_s) + N_s R_s (I_L / N_p))}{n_2 V_t N_s}\right) - 1 \right] - \left(\frac{((V_L / N_s) + N_s R_s (I_L / N_p))}{R_{sh} (N_s / N_p)} \right) \quad (9)$$

$$I_L = I_{ph} N_p - I_{s1} N_p \left[\exp\left(\frac{q((V_L / N_s) + N_s R_s (I_L / N_p))}{n_1 V_t N_s}\right) - 1 \right] - I_{s2} N_p \left[\exp\left(\frac{q((V_L / N_s) + N_s R_s (I_L / N_p))}{n_2 V_t N_s}\right) - 1 \right] - I_{s3} N_p \left[\exp\left(\frac{q((V_L / N_s) + N_s R_s (I_L / N_p))}{n_3 V_t N_s}\right) - 1 \right] - \left(\frac{((V_L / N_s) + N_s R_s (I_L / N_p))}{R_{sh} (N_s / N_p)} \right) \quad (10)$$

2.3. Problem Formulation

The problem of identifying unknown parameters for all models of PV cells and modules can be solved by converting it into an optimization problem.

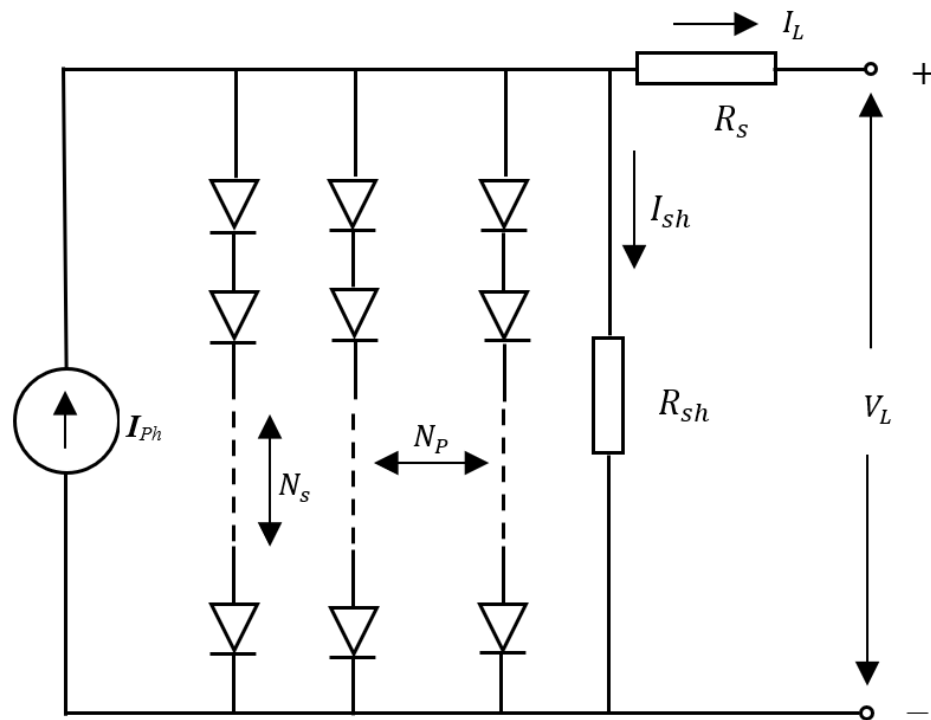


Figure 4. Equivalent circuit of the PV module.

The discrepancy between calculated and measured data is minimized during the optimization phase. The objective function is designed to find the optimal values of the unknown parameters of different models in terms of root mean square error (RMSE) [40]. It is expressed as follows:

$$RMSE(x) = \sqrt{\frac{1}{N} \sum_1^N f_M(V_L, I_L, x)} \tag{11}$$

where: N denotes collected experimental data, V_L and I_L are measured voltage and measured current, respectively. x is the solution vector. f_M is the error function, which is defined for different PV models as follows:

2.3.1. For 1DM of PV Cell

$$\begin{cases} f(V_L, I_L, x) = I_{ph} - I_{s1} \left[\exp\left(\frac{q(V_L + R_s I_L)}{n_1 K T}\right) - 1 \right] - \frac{(V_L + R_s I_L)}{R_{sh}} - I_L \\ x = \{I_{ph}, I_{s1}, R_s, R_{sh}, n_1\} \end{cases} \tag{12}$$

There are five parameters in the equation expressed above that need to be identified: I_{ph} , I_{s1} , R_s , R_{sh} and n_1 .

2.3.2. For 2DM of PV Cell

$$\begin{cases} f(V_L, I_L, x) = I_{ph} - I_{s1} \left[\exp\left(\frac{q(V_L + R_s I_L)}{n_1 K T}\right) - 1 \right] - I_{s2} \left[\exp\left(\frac{q(V_L + R_s I_L)}{n_2 K T}\right) - 1 \right] - \frac{(V_L + R_s I_L)}{R_{sh}} - I_L \\ x = \{I_{ph}, I_{s1}, I_{s2}, R_s, R_{sh}, n_1, n_2\} \end{cases} \tag{13}$$

There are seven parameters in the above equation which need to be identified: I_{ph} , I_{s1} , I_{s2} , R_s , R_{sh} , n_1 and n_2 .

2.3.3. For 3DM of PV Cell

$$\left\{ \begin{aligned} f(V_L, I_L, x) &= I_{ph} - I_{s1} \left[\exp\left(\frac{q(V_L + R_s I_L)}{n_1 K T}\right) - 1 \right] - I_{s2} \left[\exp\left(\frac{q(V_L + R_s I_L)}{n_2 K T}\right) - 1 \right] - I_{s3} \left[\exp\left(\frac{q(V_L + R_s I_L)}{n_3 K T}\right) - 1 \right] \\ &\quad - \frac{(V_L + R_s I_L)}{R_{sh}} - I_L \\ x &= \{ I_{ph}, I_{s1}, I_{s2}, I_{s3}, R_s, R_{sh}, n_1, n_2, n_3 \} \end{aligned} \right. \tag{14}$$

There are nine parameters in the last expression which need to be identified: $I_{ph}, I_{s1}, I_{s2}, I_{s3}, R_s, R_{sh}, n_1, n_2$ and n_3 .

2.3.4. For 1DM of PV Module

$$\left\{ \begin{aligned} f(V_L, I_L, x) &= N_p I_{ph} - N_p I_{s1} \left[\exp\left(\frac{q((V_L / N_s) + N_s R_s (I_L / N_p))}{n_1 V_t N_s}\right) - 1 \right] - \left[\frac{((V_L / N_s) + N_s R_s (I_L / N_p))}{R_{sh}} \right] - I_L \\ x &= \{ I_{ph}, I_{s1}, R_s, R_{sh}, n_1 \} \end{aligned} \right. \tag{15}$$

2.3.5. For 2DM of PV Module

$$\left\{ \begin{aligned} f(V_L, I_L, x) &= N_p I_{ph} - N_p I_{s1} \left[\exp\left(\frac{q((V_L / N_s) + N_s R_s (I_L / N_p))}{n_1 V_t N_s}\right) - 1 \right] - N_p I_{s2} \left[\exp\left(\frac{q((V_L / N_s) + N_s R_s (I_L / N_p))}{n_2 V_t N_s}\right) - 1 \right] \\ &\quad - \left[\frac{((V_L / N_s) + N_s R_s (I_L / N_p))}{R_{sh}} \right] - I_L \\ x &= \{ I_{ph}, I_{s1}, I_{s2}, R_s, R_{sh}, n_1, n_2 \} \end{aligned} \right. \tag{16}$$

2.3.6. For 3DM of PV Module

$$\left\{ \begin{aligned} f(V_L, I_L, x) &= N_p I_{ph} - N_p I_{s1} \left[\exp\left(\frac{q((V_L / N_s) + N_s R_s (I_L / N_p))}{n_1 V_t N_s}\right) - 1 \right] - N_p I_{s2} \left[\exp\left(\frac{q((V_L / N_s) + N_s R_s (I_L / N_p))}{n_2 V_t N_s}\right) - 1 \right] - N_p I_{s3} \left[\exp\left(\frac{q((V_L / N_s) + N_s R_s (I_L / N_p))}{n_3 V_t N_s}\right) - 1 \right] \\ &\quad - \left[\frac{((V_L / N_s) + N_s R_s (I_L / N_p))}{R_{sh}} \right] - I_L \\ x &= \{ I_{ph}, I_{s1}, I_{s2}, I_{s3}, R_s, R_{sh}, n_1, n_2, n_3 \} \end{aligned} \right. \tag{17}$$

There are five, seven and nine parameters for the three models of the PV module which must be identified, they are presented in vector x .

3. The Proposed Hybrid BB-TLBO Algorithm

In this section, the hybrid proposed algorithm is introduced, which combines biogeography-based optimization (BBO) and teaching-learning based optimization (TLBO). A brief discussion of the BBO and TLBO algorithms. Following that, the innovative hybrid algorithm, BB-TLBO, is discussed in detail, which leverages the strengths of both BBO and TLBO to enhance optimization performance.

3.1. Biogeography-Based Optimization

Biogeography-based optimization (BBO) is a metaheuristic algorithm announced by Dan Simon in the year 2008 that is inspired by the theory of island biogeography. This theory employs mathematical models to describe the patterns of migration, speciation, and extinction of species across different islands. Biogeography-based optimization (BBO) considers each individual in the population as an island with a habitat suitability index (HSI), where each variable of the island is referred to as a suitability index variable (SIV). A desirable solution is indicated by an island with a high HSI that hosts a diverse range of species, while an undesirable solution is represented by an island with a low HSI, which has a small number of species. Consequently, individuals located on high HSI islands are

more likely to migrate to islands with low HSI, and the low HSI islands receive immigrants from high HSI islands to promote genetic diversity and improve the overall quality of the population. BBO employs two operators namely migration and mutation to evolve the population [30–32].

3.1.1. Migration

Biogeography-based optimization involves assigning unique immigration λ and emigration rates μ to each island in the population, which are the functions of species in the habitat. The functions of the immigration rate and emigration rate can be defined as:

$$\lambda_s = I \left(1 - \frac{s}{N_p} \right) \tag{18}$$

$$\mu_s = E \left(\frac{s}{N_p} \right) \tag{19}$$

The maximum possible immigration rate (denoted by I) is achieved when an island has no species present, whereas the maximum emigration rate (denoted by E) occurs when the island has the maximum number of species. s is the number of species of the s^{th} individual in the ordered population according to fitness, and N_p is the number of candidate solutions in the population. With I and E typically being set to 1. Where the immigration rate (λ) determines whether a selected solution should modify its suitability index variable (SIV), while the emigration rate (μ) determines which solutions should migrate a random SIV to the selected solution.

3.1.2. Mutation

Nature is subject to cataclysmic events that can significantly alter the solution of an island, resulting in sudden changes to its habitat suitability index (HSI). In order to incorporate this type of random variation into the BBO algorithm, a mutation process is introduced, with mutation rates determined based on the species count probabilities. Specifically, the species count probability $P(s)$ represents the probability that an island contains s species, and its change rate can be calculated as:

$$\dot{P} = \begin{cases} -(\lambda_s + \mu_s)P_s + \mu_{s+1}P_{s+1}, & s = 0 \\ -(\lambda_s + \mu_s)P_s + \lambda_{s+1}P_{s-1} + \mu_{s+1}P_{s+1}, & 1 \leq s \leq s_{max} - 1 \\ -(\lambda_s + \mu_s)P_s + \lambda_{s+1}P_{s-1}, & s = s_{max} \end{cases} \tag{20}$$

where λ_s denotes the immigration rate and μ_s denotes the emigration rate when there are S species on the island, and S_{max} denotes the maximal species on the island.

The mutation rate for each solution is determined based on its respective species count probability. Solutions with a lower probability (P_s) are more likely to undergo mutations to different solutions, while those with a higher probability are less likely to experience mutations that lead to different solutions. The mutation rates can be proportional to the species count probabilities as:

$$m(S) = m_{max} \left(\frac{1 - P_s}{P_{max}} \right) \tag{21}$$

where m_{max} is the maximal mutation rate defined by the user, and P_{max} is the maximal species count probability. The mutation operator is implemented to enhance the genetic diversity of the population, providing a means to improve solutions for islands with a low habitat suitability index (HSI), while allowing high HSI islands to potentially achieve even better solutions. In essence, the mutation operator helps to balance out the population and promote progress towards an optimal solution for the given problem.

3.2. Teaching–Learning–Based Optimization

TLBO is a population-based evolutionary algorithm that was proposed recently by Rao et al., and its main idea is to simulate a classical learning process that consists of a teacher phase and a learner phase. In the teacher phase, the best solution found in the entire population is considered as the teacher, and it shares its knowledge with the students to improve their outputs (i.e., grades or marks). In the learner phase, the students also learn knowledge from each other to improve their outputs. TLBO conducts this process through two basic operations, the teacher phase and the learner phase [2,3,41–44].

3.2.1. Teacher Phase

During the teacher phase, the best learner discovered so far is selected as the teacher based on their fitness value. Additionally, the average position of all the learners must be computed to update the positions of every learner. Assuming that X_i represents the position of the i^{th} learner in an n -dimensional optimization problem, then X_i can be expressed as:

$$X_i = \{x_{i1}, x_{i2}, \dots, x_{in}\} \tag{22}$$

The teaching process is formulated as follows:

$$X_{new,i} = X_{old,i} + rand() * (X_{Teacher} - TF * X_{mean}) \tag{23}$$

The variables and computations utilized in the teacher phase include $X_{new,i}$ and $X_{old,i}$, which represent the new and old positions, respectively, of the i^{th} learner. $X_{Teacher}$ denotes the position of the current teacher, while X_{mean} is the mean position of the current class, calculated as the sum of all learners' positions divided by the total number of students (N_p) (As it is shown in Equation (24)). The function $rand()$ generates a random number within the range $[0, 1]$, and TF denotes the teaching factor, which is typically set to either 1 or 2 using a heuristic approach.

It is necessary to re-evaluate all learners after each iteration of the teacher phase. If the new position $X_{new,i}$ is better than the old position $X_{old,i}$, it will be accepted and will flow into the learner phase. Otherwise, $X_{old,i}$ will not be updated.

$$X_{mean} = \frac{1}{N_p} \sum_{i=1}^{N_p} X_i \tag{24}$$

3.2.2. Learner Phase

During the learner phase, the i^{th} learner X_i is randomly paired with another learner X_j from the class who is distinct from X_i . The learning process is described as follows:

$$X_{new,i} = \begin{cases} X_{old,i} + rand() * (X_{old,i} - X_{old,j}), & \text{if } f(X_{old,i}) < f(X_{old,j}) \\ X_{old,i} + rand() * (X_{old,j} - X_{old,i}), & \text{otherwise} \end{cases} \tag{25}$$

In this context, $X_{new,i}$ represents the new position of the i^{th} learner, while $X_{old,i}$ and $X_{old,j}$ correspond to the old positions of the i^{th} and j^{th} learners, respectively. Additionally, $rand()$ generates a random number between 0 and 1.

To update the learner positions, $X_{new,i}$ is accepted if it results in a better function value compared to the previous positions, $X_{old,i}$ and $X_{old,j}$.

3.3. Proposed BB-TLBO Algorithm

The BBO was applied to solve many optimization problems, and it proves its efficiency in finding optimal solutions. This is due to its good exploration feature for the current population. Nevertheless, BBO suffers from some drawbacks such as poorness in

exploitation features, negligence of the best individuals over generations, and generation of infeasible solutions.

In contrast, the TLBO algorithm is known as a new and simple-to-understand method. Because of its design which mimics the school strategy in learning. However, TLBO suffers from deficiencies such as trapping in local optima and poor population diversity.

To overcome the over mentioned disadvantages, a new hybrid BB-TLBO algorithm is proposed in this paper. The BB-TLBO is described through the following phase:

3.3.1. Initialization

The population in the BB-TLBO are considered learners in class $\{X_1, X_2, \dots, X_{N_p}\}$. The initialization of the BB-TLBO is inspired by the BBO technique where an assignment of positions is performed randomly to each individual along with the search space. Each individual position is represented by a vector X_i .

3.3.2. Migration Process

In this phase, each individual (learner) changes his position inside the class to enhance his level of knowledge. This movement is performed using the immigration and an emigration rate represented by λ and μ respectively, using Equations (18) and (19).

3.3.3. Teaching Phase

After performing the migration process, the next step (inspired by the TLBO) is to calculate the mean level of knowledge in the class using Equation (24).

The population is then sorted in descending order from the best to the worst according to their fitness. X_1 is selected as teacher, and the rest of the population is considered as learners. The teaching phase aims to enhance the mean level of knowledge of learners. Each learner X_j will update his knowledge level using Equation (23).

After evaluation, if the fitness of $X_{new,i}$ is better than the fitness of $X_{old,i}$ then $X_{new,i}$ replaces $X_{old,i}$ and is accepted for pursuing the learning phase, otherwise $X_{old,i}$ stays in its current position.

3.3.4. Learning Phase

The learning process is characterized by sharing knowledge between each learner X_i and other X_j that is randomly selected among the population. This phase is mathematically expressed as Equation (25):

After evaluating the fitness of $X_{new,i}$, $X_{new,i}$ replaces $X_{old,i}$ if it has a better fitness, otherwise $X_{old,i}$ stays in its current position. At the end of this phase, a sorting of the current population is performed.

3.3.5. Elitism Phase

The final step in BB-TLBO is the elitism process, which is taken from the BBO. Here, a predefined keeping rate K_r is used to select the best individuals among the current population to be considered for the next iteration. The elitism process is expressed through the following equation:

$$X_s = \begin{cases} X_{N_p-s+i} & \text{if } s < \text{round}(K_r * N_p) \\ X_s & \text{if } s > \text{round}(K_r * N_p) \end{cases} \quad (26)$$

where X_s is the individual being selected to take part in the next generation. i denotes the current iteration. After reaching the termination criterion, the algorithm returns X^* as the optimal solution.

3.4. Pseudocode of the BB-TLBO Algorithm

The pseudocode of the BB-TLBO algorithm (Algorithm 1) is given below and its flowchart is presented in Figure 5.

Algorithm 1: Pseudocode of the BB-TLBO Algorithm

- 1: Define problem aspects: *Fitness function $f(x)$, Dimension D ; Search space boundaries; Maximum number of iterations.*
- 2: Set algorithm parameters: *Number of populations N_p ; Keeping rate K_r ; Immigration rates λ ; emigration rate μ .*
- 3: Generate a random set of habitats (learners)
- 4: **for** $it = 1: It_Max$ **do**
- 5: **for** $i = 1$ to N_p **do**
- 6: **for** $k: 1$ to D **do**
- 7: **if** $rand \leq \lambda_i$ **then**
- 8: Assign rate of immigration λ_i and emigration μ_i to each candidate X_i using Equations (18) and (19)
- 9: **end if**
- 10: **end for**
- 11: Calculate the mean level of knowledge using Equation (24)
- 12: Sort the current population from the best to the worst
- 13: Set the best individual as a teacher
- 14: Update knowledge level of each learner using Equation (23) (teaching phase)
- 15: Update knowledge level of each learner using Equation (25) (learning phase)
- 16: Sort the new population from the best to the worst
- 17: Select the next generation population by using Equation (26) (Elitism)
- 18: **End for**
- 19: **End for**

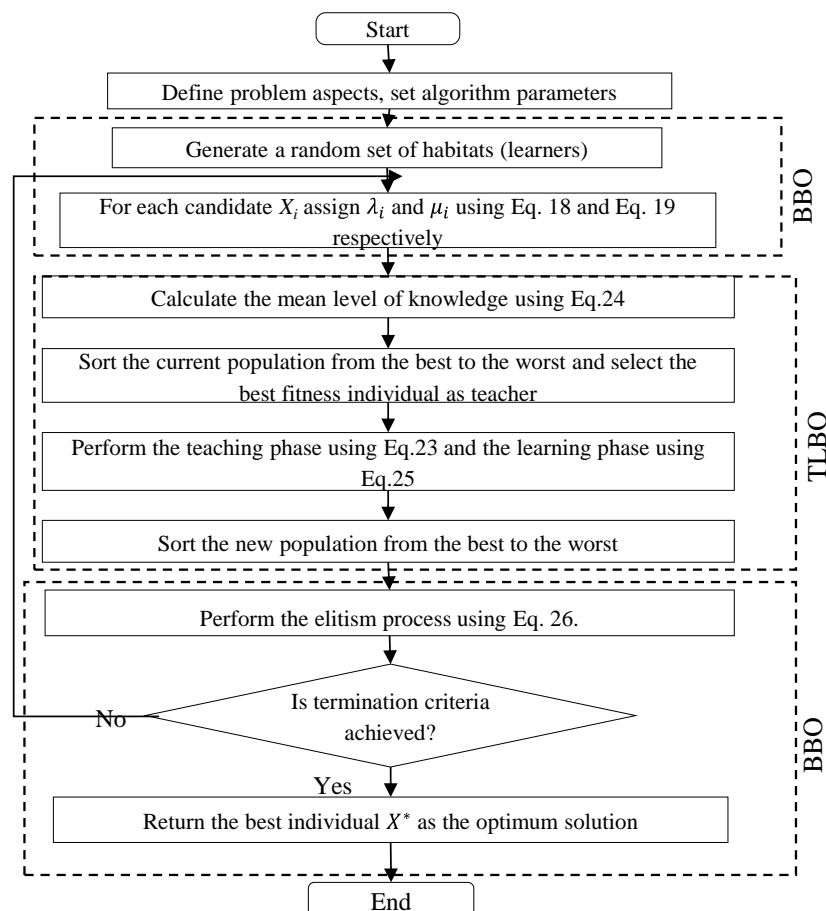


Figure 5. Flowchart of BB-TLBO algorithm.

4. Results and Discussion

This section is dedicated to the discussion of the experimental results obtained and the verification of the performance of the proposed hybrid algorithm.

In order to solve the parameter extraction problem, this algorithm is tested on two different cases, namely: the RTC FRANCE silicon solar cell and the commercial PV solar modules: the monocrystalline STM6-40/36 with their three different models (1DM, 2DM and 3DM).

To collect the experimental data I-V, 26 pairs of voltage and current samples were taken from a 57 mm diameter RTC France silicon solar cell at 33 °C and 1000 W/m² solar irradiance in order to extract the unknown parameters of three models (1DM, 2DM and 3DM) [45] as shown in Appendix A.

Likewise, 20 pairs of voltage and current data sets were collected from the STM6-40/36 module under the cell temperature of 51 °C and solar irradiation of 1000 W/m² [45] as shown in Appendix A.

The lower and the upper limits (LL and UL) of the parameters of the three different models (1DM, 2DM and 3DM) are shown in Table 1 [46].

Table 1. Upper and lower limits of the 1DM, 2DM and 3DM parameters.

		RTC France Solar Cell		STM6-40/36	
	Parameters	LL	UL	LL	UL
1DM	$I_{ph}(A)$	0	1	0	2
	$I_{s1}(A)$	0	1×10^{-6}	0	50×10^{-6}
	$R_s(\Omega)$	0	0.5	0	0.36
	$R_{sh}(\Omega)$	0	100	0	1000
	n_1	1	2	1	2
2DM	$I_{ph}(A)$	0	1	0	2
	$I_{s1}, I_{s2}(A)$	0	1×10^{-6}	0	50×10^{-6}
	$R_s(\Omega)$	0	0.5	0	0.36
	$R_{sh}(\Omega)$	0	100	0	1000
	n_1, n_2	1	2	1	2
3DM	$I_{ph}(A)$	0	1	0	2
	$I_{s1}, I_{s2}, I_{s3}(A)$	0	1×10^{-6}	0	50×10^{-6}
	$R_s(\Omega)$	0	0.5	0	0.36
	$R_{sh}(\Omega)$	0	100	0	1000
	n_1, n_2, n_3	1	2	1	2
		2	5	1	2

To verify the efficiency of the proposed hybrid algorithm, it was compared to other benchmarked methods such as DOLADE, LAPSO, ABC, BBO, TLBO, IQSODE, etc.

Each algorithm had been executed several times (in this example 30 executions) so that they could start their exploration from the same random point in the search space.

The simulation was performed in MATLAB 2019b, Intel(R) Core (TM) i3-6600U CPU@2.60 GHz 2.81 GHz.

4.1. Accuracy Analysis

4.1.1. RTC France Silicon Solar Cell Identification

For the RTC France silicon solar cell, Table 2 presents the results of the identification of five, seven and nine parameters as well as the RMSE values of the 1DM, 2DM and 3DM obtained by the proposed algorithm BB-TLBO and other metaheuristic algorithms.

Table 2. Best values of the identified parameters for the three adopted models of the RTC France silicon solar cell.

Ref.		$I_{ph}(A)$	$I_{s1}(A)$	$I_{s2}(A)$	$I_{s2}(A)$	$R_s(\Omega)$	$R_{sh}(\Omega)$	n_1	n_2	n_3	RMSE
1DM											
[29]	DOLADE	0.760776	3.230208×10^{-7}	/	/	0.036377093	53.7185226	1.48118359	/	/	9.860219×10^{-4}
[45]	GWOCs	0.76077	3.21920×10^{-7}	/	/	0.03639	53.632	1.4808	/	/	9.860700×10^{-4}
[47]	OLBGWO	0.760775	3.23023×10^{-7}	/	/	0.036377	53.718849	1.481184	/	/	9.860220×10^{-4}
[48]	PSO	0.7682	3.30180×10^{-7}	/	/	0.03624	53.59878	1.48334	/	/	9.861450×10^{-4}
[49]	IMFOL	0.760776	3.23021×10^{-13}	/	/	0.036377092	53.7185307	1.4811836	/	/	9.860219×10^{-4}
[49]	MFO	0.760656	4.22288×10^{-13}	/	/	0.035295103	62.2888994	1.50865857	/	/	1.111629×10^{-3}
[50]	LNMHGS	0.760758	3.35381×10^{-7}	/	/	0.0362279	54.7669545	1.48497347	/	/	9.886170×10^{-4}
[51]	HsOA	0.760763	3.32135×10^{-7}	/	/	0.036266569	54.4885001	1.48399009	/	/	9.874471×10^{-4}
[52]	IQSODE	0.760776	3.23021×10^{-7}	/	/	0.036377093	53.7185251	1.48118359	/	/	9.860219×10^{-4}
[53]	RUN	0.760611	3.20×10^{-7}	/	/	0.03641606	53.6707057	1.4802504	/	/	9.8624×10^{-4}
[54]	RLDE	0.76078	3.230200×10^{-7}	/	/	0.03638	53.71853	1.48118	/	/	9.860220×10^{-4}
[54]	FLIDE	0.76078	3.230200×10^{-7}	/	/	0.03638	53.71852	1.48118	/	/	9.860220×10^{-4}
[54]	LAPSO	0.76078	3.230200×10^{-7}	/	/	0.03638	53.71852	1.48118	/	/	9.86022×10^{-4}
	BBO	0.76073	3.665000×10^{-7}	/	/	0.0356482	54.81141	1.49407	/	/	1.060180×10^{-3}
	TLBO	0.7601	4.226240×10^{-7}	/	/	0.0351926	63.40126	1.50879	/	/	9.868560×10^{-4}
proposed	BB-TLBO	0.760776	3.23021×10^{-7}	/	/	3.63771×10^{-2}	53.7186	1.48118084	/	/	9.860219×10^{-4}
2DM											
[48]	GWOCs	0.76076	5.377200×10^{-7}	2.485500×10^{-7}	/	0.03666	54.7331	2	1.4588	/	9.833400×10^{-4}
[48]	OLBGWO	0.760781	2.259390×10^{-7}	6.431510×10^{-7}	/	0.036722	55.307755	1.451328	1.96175	/	9.825560×10^{-4}
[48]	CWOA	0.76077	2.415000×10^{-7}	6.000000×10^{-7}	/	0.03666	55.2016	1.45651	1.9899	/	9.827200×10^{-4}
[29]	DOLADE	0.760781	2.259740×10^{-7}	7.493490×10^{-7}	/	0.03674	55.4854	1.45102	2	/	9.824849×10^{-4}
[49]	IMFOL	0.760779	7.663201×10^{-13}	3.673056×10^{-8}	/	55.6567344	2	2.2515×10^{-7}	1.4507788	/	9.825250×10^{-4}
[53]	RUN	0.7608025	2.60×10^{-7}	5.58×10^{-7}	/	0.03644583	55.3832189	1.46347838	1.9996951	/	9.8717×10^{-4}
[49]	MFO	0.760693	2.481684×10^{-13}	3.604705×10^{-8}	/	62.55984	1.461875	0.000001	2	/	1.053209×10^{-3}
[52]	IQSODE	0.760781	7.493445×10^{-7}	2.259746×10^{-7}	/	0.036740429	55.4854438	2	1.4510169	/	9.824849×10^{-4}
[54]	RLDE	0.76078	2.259700×10^{-7}	7.493500×10^{-7}	/	0.03674	55.48544	1.45102	2	/	9.824850×10^{-4}
[54]	FLIDE	0.76078	7.493500×10^{-7}	2.259700×10^{-7}	/	0.03674	55.48542	2	1.45102	/	9.824850×10^{-4}
[54]	LAPSO	0.76078	7.493500×10^{-7}	2.259700×10^{-7}	/	0.03674	55.48545	2	1.45102	/	9.82485×10^{-4}
	BBO	0.76083	1.000000×10^{-6}	9.997310×10^{-7}	/	0.0287533	100	1.62607	1.85384	/	1.130320×10^{-3}
	TLBO	0.76065	4.636840×10^{-7}	8.371750×10^{-10}	/	0.0348009	64.1189	1.51873	1.62049	/	1.004280×10^{-3}
proposed	BB-TLBO	0.760781	7.48262×10^{-7}	2.26102×10^{-7}	/	0.036739843	55.48268484	2	1.451061106	/	9.824848×10^{-4}
3DM											
[48]	RAO	0.760795	2.62000×10^{-13}	2.63000×10^{-13}	9.780000×10^{-13}	0.03674	55.35801	1.771502	1.451415	2.41101	9.84569×10^{-4}
[48]	TLO	0.760789	2.54000×10^{-13}	4.56000×10^{-14}	1.480000×10^{-13}	0.03671	55.3144	1.460287	1.740863	2.25143	9.86125×10^{-4}
[53]	RUN	0.760836723	3.30×10^{-12}	2.65×10^{-7}	8.42×10^{-8}	0.36313464	53.61258389	1.071707	1.47338	1.572965	9.89133×10^{-4}
[48]	CS	0.760776	1.40000×10^{-7}	1.90000×10^{-7}	3.100000×10^{-8}	0.0363	53.7218	1.4872	1.4771	4.4663	9.87857×10^{-4}
[48]	R-II	0.760792	2.60000×10^{-7}	5.60000×10^{-12}	5.700000×10^{-7}	0.0366	54.9149	1.4608	1.1466	2.0208	9.80467×10^{-4}
	BBO	0.76172	4.88556×10^{-7}	6.61964×10^{-7}	1.91131×10^{-7}	0.03082	46.52017159	1.88106	1.56784	2	1.22456×10^{-3}
	TLBO	0.76071	3.51523×10^{-7}	1.54967×10^{-9}	7.49560×10^{-7}	0.0359163	55.36847	1.489839	1.967693	3.50035	9.85769×10^{-4}
proposed	BB-TLBO	0.760781	2.650936×10^{-7}	8.168814×10^{-27}	1×10^{-6}	0.036634534	55.21270072	1.46360555	2	2.2370724	9.80767×10^{-4}

- For the 1DM identification and according to the lowest RMSE value (9.860219×10^{-4}), BB-TLBO, DOLADE, IMFOL and IQSODE have the best results compared to GWOCs, OLBGWO, PSO, MFO, LNMHGS, HSOA, RLDE, FLIDE, LAPSO, BBO and TLBO.
- For the 2DM, BB-TLBO is able to reach the minimum RMSE value of 9.824848×10^{-4} , which means that they allow us to obtain the best results.
- For the 3DM, the best parameters identified were obtained by BB-TLBO (RMSE value of 9.80767×10^{-4}).

4.1.2. Monocrystalline Solar Module STM6-40/36 Identification

Table 3 reports the results of the identification of five, seven, and nine parameters for the 1DM, 2DM and 3DM respectively of the STM6-40/36 solar module obtained by BB-TLBO and other algorithms (BBO, DE, ABC, TLBO, DE/BBO, BLPSO . . .).

- As shown in Table 3, for the 1DM identification, BB-TLBO reaches the lowest RMSE value of 1.729814×10^{-3} followed by IMFOL with an RMSE value of 1.729815×10^{-3} . The TLBO-ABC identification results indicate that metaheuristic hybrid optimization algorithms demonstrate better performance than algorithms without hybridization.
- BB-TLBO obtained the lowest value of RMSE (best RMSE) which is equal to 1.693885×10^{-3} for 2DM and 1.689064×10^{-3} for 3DM compared to other algorithms mentioned in the same table.
- The MCSWOA provides the second-best RMSE value (1.706100×10^{-3}) for 2DM and SDO provides the second-best RMSE value of 1.701880×10^{-3} for 3DM.

After identifying the parameters of all models for RTC France silicone solar cell and STM6-40/36 solar module, the output current and power relative to the measured voltage can be determined. Figures 6 and 7 show the IAE absolute error of current and power calculated using Equations (27) and (28), respectively.

$$IAE(I) = |I_c - I_m| \tag{27}$$

$$IAE(P) = |P_c - P_m| \tag{28}$$

where: I_c and P_c are the current and the power calculated using BB-TLBO, respectively. I_m and P_m are the measured current and power, respectively.

As can be seen in Figures 6 and 7, the current IAE value for:

- RTC France solar cells based on 1DM, 2DM and 3DM are less than 0.0025(A), 0.002896(A) and 0.00310(A), respectively.
- STM6-40/36 solar module are less than 0.00609(A), 0.005581(A) and 0.005513(A) for 1DM, 2DM and 3DM, respectively.

As can be shown in Figures 6 and 7, The value of IAE of the power for:

- RTC France solar cells based on 1DM, 2DM and 3DM are less than 0.0014583(w), 0.001413(w) and 0.001813554(w).
- STM6-40/36 solar module are less than 0.09062(w), 0.083042(w) and 0.082039(w) for 1DM, 2DM and 3DM, respectively.

Moreover, the characteristic curves (I-V) and (P-V) for all the models and in the different cases show that the measured data and the calculated data obtained by BB-TLBO are similar (Figures 8 and 9).

It can be concluded from Tables 2 and 3 that the proposed hybrid metaheuristic algorithm BB-TLBO can achieve better RMSE value and exhibits very good accuracy in parameter estimation compared to other algorithms for 1DM, 2DM and 3DM whether for the RTC France solar cell or the STM6-40/36 solar module.

Table 3. Best values of the identified parameters for the three adopted models of the solar module STM6-40/36.

Ref.	Algo	$I_{ph}(A)$	$I_{s1}(A)$	$I_{s2}(A)$	$I_{s2}(A)$	$R_s(\Omega)$	$R_{sh}(\Omega)$	n_1	n_2	n_3	RMSE
1DM											
[43]	TLBO-ABC	1.66317	2.140430×10^{-6}	/	/	3.63×10^{-3}	17.25952	1.54354	/	/	1.806100×10^{-3}
[45]	GWO	1.656206	7.344000×10^{-6}	/	/	1.48×10^{-3}	930.331	1.69641	/	/	7.141200×10^{-3}
[32]	CS	1.66172	3.728150×10^{-6}	/	/	1.73×10^{-3}	21.74472	1.60905	/	/	2.515900×10^{-3}
[45]	GWCS	1.6641	1.744900×10^{-6}	/	/	4.24×10^{-3}	15.7326	1.5207	/	/	1.733700×10^{-3}
[49]	IMFOL	1.6639175	1.729858×10^{-6}	/	/	0.15443712	572.509298	55.74263	/	/	1.729815×10^{-3}
[49]	MFO	1.8623975	0	/	/	0	32.8634387	27.04247	/	/	3.107574×10^{-1}
[49]	LNMHGS	1.6634534	2.084166×10^{-6}	/	/	0.1327753	608.102259	56.5036	/	/	1.781552×10^{-3}
[49]	HSGA	1.6629825	2.511230×10^{-6}	/	/	0.11062102	649.583949	57.28595	/	/	1.935188×10^{-3}
	BBO	1.66096	5.412135×10^{-6}	/	/	0.00035139	25.84391774	1.656222	/	/	2.301350×10^{-3}
	TLBO	1.6636873	1.781895×10^{-6}	/	/	0.0041756	16.09665216	1.523005	/	/	2.141840×10^{-3}
proposed	BB-TLBO	1.6639048	1.73866×10^{-6}	/	/	4.27377×10^{-3}	15.92829602	1.5203	/	/	1.729814×10^{-3}
2DM											
[55]	ELPSO	1.664843	6.210924×10^{-6}	1.670100×10^{-9}	/	0.5	606.8883	41.99348	67.344	/	1.830700×10^{-3}
[56]	MCSWOA	1.6639	6.103000×10^{-7}	1.176290×10^{-5}	/	0.0054	16.9519	1.4224	2.1992	/	1.706100×10^{-3}
[57]	SDO	1.6639	1.738500×10^{-6}	4.999850×10^{-5}	/	0.0043	15.9372	1.5203	54.5816	/	1.729800×10^{-3}
[21]	EPSO	1.6644	7.401100×10^{-6}	1.433800×10^{-6}	/	0.26591	560.55	1.7577	/	/	2.057300×10^{-3}
	BBO	1.6738728	5.703159×10^{-6}	2.357689×10^{-5}	/	4.75×10^{-7}	384.0411249	1.931814	1.908805	/	3.292930×10^{-3}
	TLBO	1.6638699	1.455541×10^{-6}	5.277084×10^{-7}	/	0.00425743	16.1306678	1.508304	1.708518	/	1.891110×10^{-3}
proposed	BB-TLBO	1.6637441	5.784671×10^{-8}	5.939555×10^{-6}	/	0.00643011	17.39713593	1.255163	1.80345	/	1.693885×10^{-3}
3DM											
[40]	BSDE	1.6610885	1.489080×10^{-6}	3.903720×10^{-6}	1.365650×10^{-6}	0.00201029	25.78757895	1.531215	1.868278	1.882878	2.894519×10^{-3}
[40]	SDO	1.6637443	6.359330×10^{-6}	8.339200×10^{-7}	4.720130×10^{-7}	0.00537714	17.00997277	1.995203	1.969208	1.404689	1.701880×10^{-3}
[40]	MRFO	1.6623179	2.599330×10^{-6}	6.333390×10^{-8}	2.770140×10^{-7}	0.0028541	19.10015605	1.566776	1.955282	1.974909	2.033192×10^{-3}
[40]	BSA	1.6575761	3.506960×10^{-7}	2.188980×10^{-7}	1.141650×10^{-5}	0.00466652	43.38223673	1.392706	1.823212	1.969855	3.654669×10^{-3}
[40]	CSO	1.6608011	5.354570×10^{-6}	4.538900×10^{-8}	3.564310×10^{-7}	0.00011186	25.49507041	1.657277	1.999604	1.85013	3.320772×10^{-3}
	BBO	1.6550041	6.93982×10^{-9}	6.56508×10^{-9}	6.89231×10^{-9}	0.0155553	13.11044618	1.141827	1.334208	1.114979	3.366020×10^{-3}
	TLBO	1.6631291	1.68041×10^{-7}	1.97437×10^{-6}	1.20913×10^{-10}	0.00381094	17.01133833	1.997693	1.534797	1.555108	1.805210×10^{-3}
proposed	BB-TLBO	1.6637666	7.76195×10^{-7}	4.22435×10^{-6}	1.76262×10^{-8}	0.0068122	17.38999711	1.671175	1.761521	1.184057	1.689064×10^{-3}

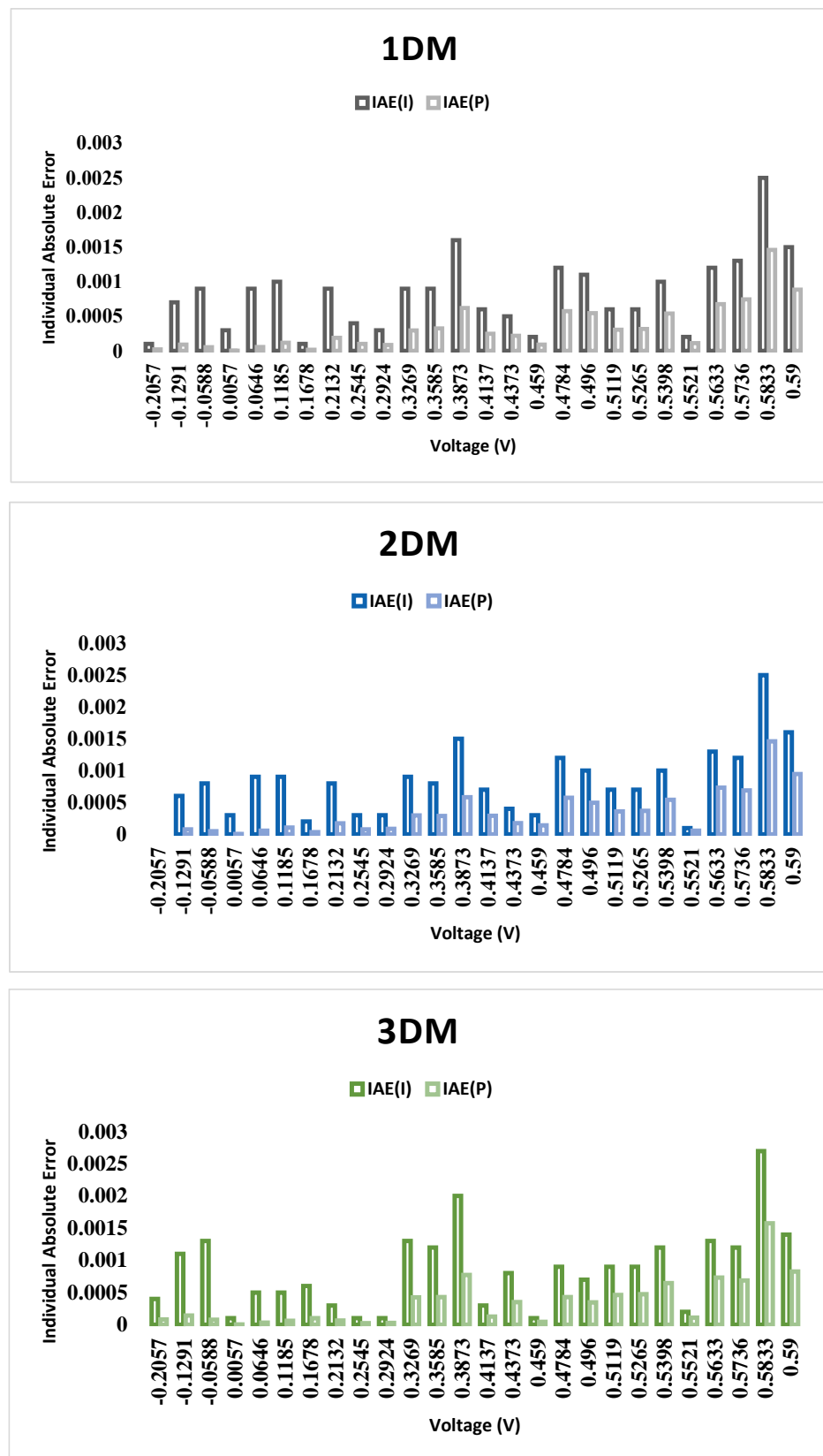


Figure 6. IAE of the current and the power of the three adopted models of the RTC France silicon solar cell.

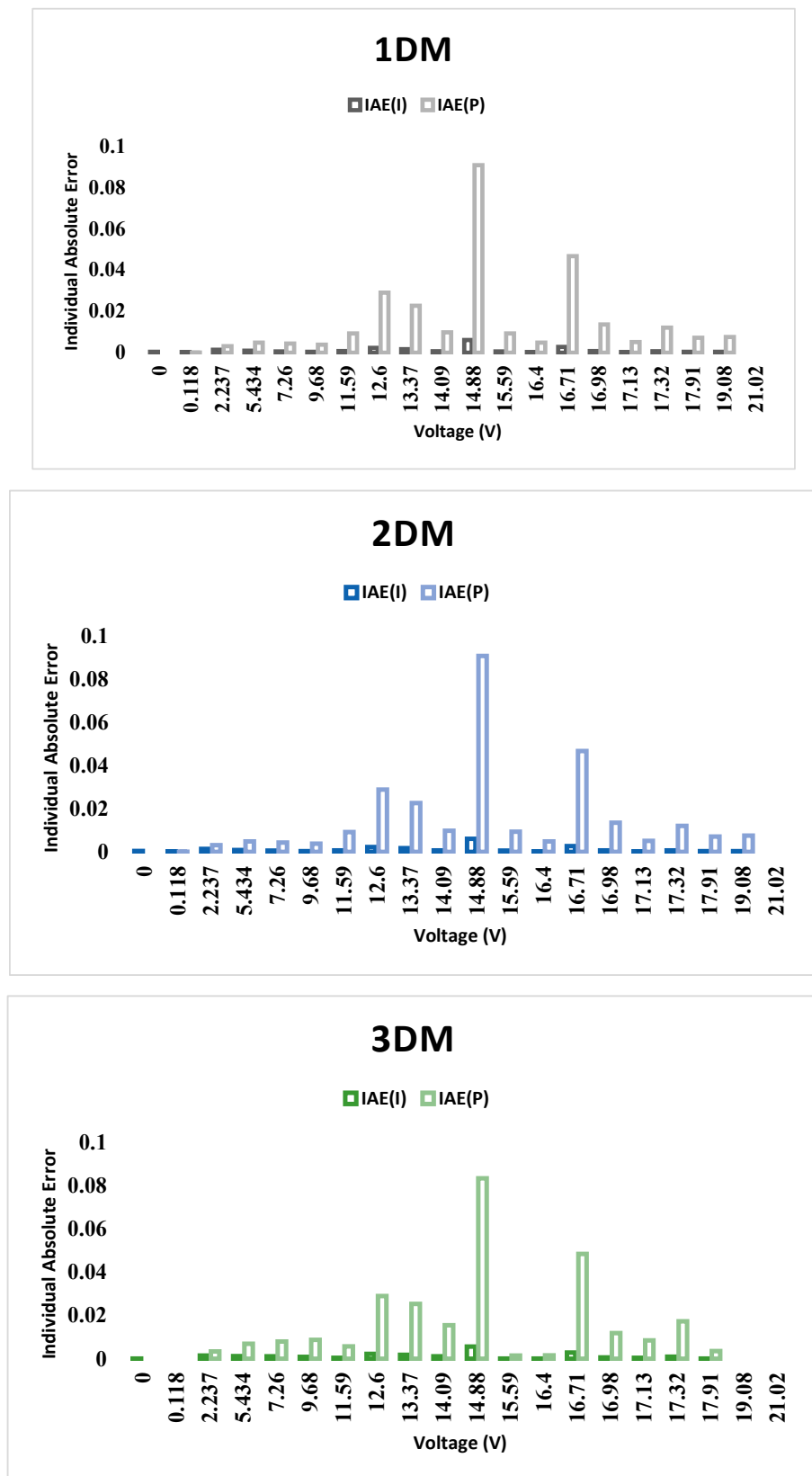


Figure 7. IAE of the current and the power of the three adopted models of the solar module STM6-40/36.

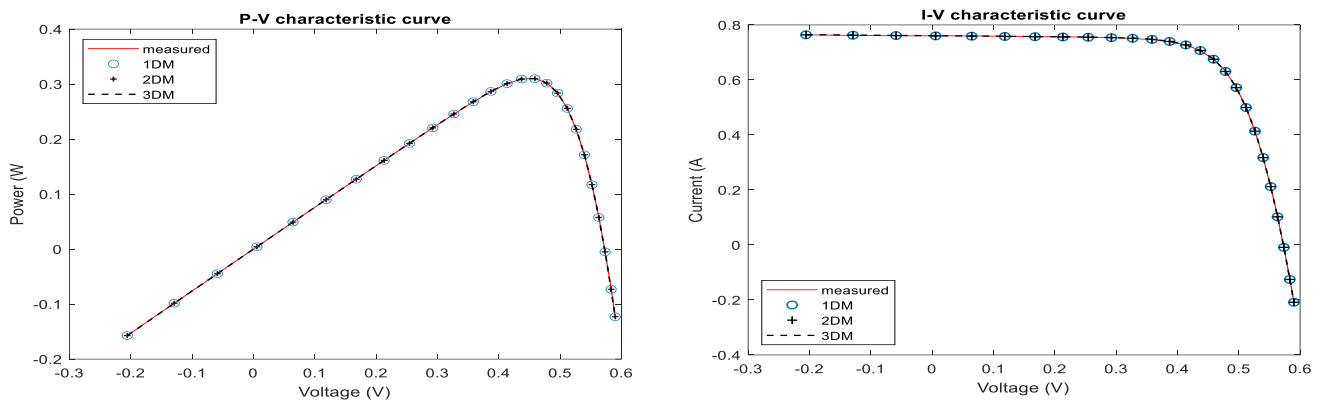


Figure 8. P-V and I-V characteristic curves for the three RTC France silicon solar cell models.

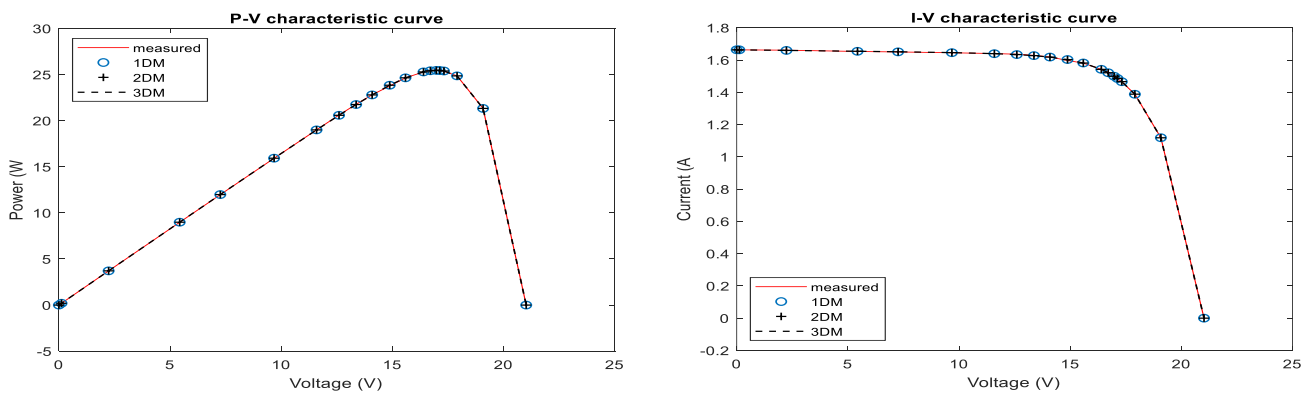


Figure 9. P-V and I-V characteristic curves for the three models of the STM6-40/36 solar modules.

4.2. Statistics Analysis

In order to evaluate the robustness and reliability of the proposed BB-TLBO algorithm, the statistical results obtained by BB-TLBO and other algorithms such as BBO, TLBO, DOLADE, LAPSO, ... are presented in Tables 4 and 5.

These results include: $RMSE_{min}$ which represents the lowest value of RMSE, $RMSE_{mean}$ corresponds to the average value of RMSE, $RMSE_{max}$ is the worst value, $It(s)$ is the number of iterations to obtain the best results, $CPU(s)$ is the running time and STD is the standard deviation of the RMSE values, it indicates the reliability of the algorithm.

The statistical results for the 1DM, 2DM and 3DM of RTC France silicon solar cells are shown in Table 4.

- For 1DM identified on the basis of BB-TLBO, it is found that the lowest RMSE value is reached after 50 iterations and in 1.14 s with an STD of 8.821895×10^{-19} .
- For the France RTC cell based on 2DM, the best results are obtained by BB-TLBO which records an $RMSE = 9.824848 \times 10^{-4}$, $STD = 2.686117 \times 10^{-8}$, $It(s) = 117$ and $CPU(s) = 10.75355$ s.
- For the identification of the 3DM of RTC France, BB-TLBO records an $RMSE = 9.807670 \times 10^{-4}$, $STD = 3.034764 \times 10^{-8}$, $It(s) = 143$ and $CPU(s) = 11.1490$ s.

For the identification of the STM6-40/36 solar module based on 1DM, 2DM and 3DM, the statistical results obtained by BB-TLBO and other algorithms are shown in Table 5.

Table 4. Statistical results obtained during the identification of 1DM, 2DM and 3DM of RTC France.

Ref.	Alg	$RMSE_{min}$	$RMSE_{mean}$	$RMSE_{max}$	STD	It(s)	CPU(s)
1DM							
[52]	ECM–JADE	9.860219×10^{-4}	9.860219×10^{-4}	9.860219×10^{-4}	4.609693×10^{-17}	/	/
[29]	DOLADE	9.860219×10^{-4}	9.860219×10^{-4}	9.860219×10^{-4}	3.277377×10^{-17}	/	/
[49]	IMFOL	9.860200×10^{-4}	9.870500×10^{-4}	9.897700×10^{-4}	1.020700×10^{-6}	/	/
[54]	RLDE	9.860220×10^{-4}	9.860220×10^{-4}	9.860220×10^{-4}	5.451690×10^{-17}	/	/
[54]	LaPSO	9.860220×10^{-4}	9.860220×10^{-4}	9.860220×10^{-4}	3.668200×10^{-13}	/	/
[49]	MFO	1.11160×10^{-3}	2.20190×10^{-3}	2.44800×10^{-3}	3.81790×10^{-4}	/	/
	BBO	1.06018×10^{-3}	2.11037×10^{-3}	2.46065×10^{-3}	4.74228×10^{-4}	>2000	>20.3542
	TLBO	9.86856×10^{-4}	1.05013×10^{-3}	1.23504×10^{-3}	6.75216×10^{-5}	>2000	>10.4671
proposed	BB-TLBO	9.860219×10^{-4}	9.860219×10^{-4}	9.860219×10^{-4}	8.821895×10^{-19}	50	1.137621
2DM							
[52]	IQSODE	9.824849×10^{-4}	9.860260×10^{-4}	9.836710×10^{-4}	1.345204×10^{-6}	/	/
[29]	DOLADE	9.824849×10^{-4}	9.860219×10^{-4}	9.826028×10^{-4}	6.457690×10^{-7}	/	/
[49]	IMFOL	9.825300×10^{-4}	9.959600×10^{-4}	9.867500×10^{-4}	3.226800×10^{-6}	/	/
[49]	MFO	1.053200×10^{-3}	2.994000×10^{-3}	2.147700×10^{-3}	4.346400×10^{-4}	/	/
[54]	FLIDE	9.824850×10^{-4}	9.884790×10^{-4}	1.021620×10^{-3}	1.055370×10^{-5}	/	/
[54]	RLDE	9.824850×10^{-4}	9.858400×10^{-4}	1.007730×10^{-3}	4.400270×10^{-6}	/	/
[54]	LaPSO	9.862120×10^{-4}	9.824850×10^{-4}	9.842650×10^{-4}	1.680880×10^{-6}	/	/
	BBO	1.13032×10^{-3}	2.45570×10^{-3}	3.72398×10^{-3}	7.68496×10^{-4}	>2000	>20.2376
	TLBO	1.00428×10^{-3}	1.12907×10^{-3}	1.38165×10^{-3}	1.11267×10^{-4}	>2000	>22.34672
proposed	BB-TLBO	9.824848×10^{-4}	9.824899×10^{-4}	9.826319×10^{-4}	2.683117×10^{-8}	117	10.75355
3DM							
[58]	CS	9.87857×10^{-4}	3.51602×10^{-3}	8.49868×10^{-1}	2.28842×10^{-3}	/	/
[48]	TLO	9.86125×10^{-4}	2.92145×10^{-3}	4.41563×10^{-1}	2.19458×10^{-3}	/	/
[48]	RAO	9.84569×10^{-4}	2.01125×10^{-3}	2.12589×10^{-1}	9.62140×10^{-4}	/	/
[48]	ABC	9.84522×10^{-4}	3.51369×10^{-3}	8.52365×10^{-1}	2.28412×10^{-3}	/	/
	BBO	1.22456×10^{-3}	2.36534×10^{-3}	3.68666×10^{-3}	6.53851×10^{-4}	>2000	>8.7465
	TLBO	9.85769×10^{-4}	1.04152×10^{-3}	1.16712×10^{-3}	5.44385×10^{-5}	>2000	>9.2232857
proposed	BB-TLBO	9.807670×10^{-4}	9.807670×10^{-4}	9.807670×10^{-4}	3.034764×10^{-8}	143	11.1490

Table 5. Statistical results obtained during the identification of 1DM, 2DM and 3DM of the STM6-40/36 solar module.

Ref.	Alg	$RMSE_{min}$	$RMSE_{mean}$	$RMSE_{max}$	STD	It(s)	CPU(s)
1DM							
[59]	MLBSA	1.743415×10^{-3}	4.297333×10^{-3}	3.329609×10^{-2}	5.677849×10^{-3}	/	/
[45]	GWOCs	1.733700×10^{-3}	1.745700×10^{-3}	1.752800×10^{-3}	1.044700×10^{-5}	/	/
[55]	ELPSO	2.180300×10^{-3}	2.250300×10^{-3}	3.716000×10^{-3}	2.921100×10^{-4}	/	/
[57]	SDO	1.729800×10^{-3}	1.770300×10^{-3}	1.950000×10^{-3}	4.510800×10^{-5}	/	/
[49]	IMFOL	1.887000×10^{-3}	3.033500×10^{-3}	4.674900×10^{-3}	8.545400×10^{-4}	/	/
[49]	MFO	3.107600×10^{-1}	3.107600×10^{-1}	3.107600×10^{-1}	1.693800×10^{-16}	/	/
[52]	IQSODE	1.729814×10^{-3}	1.729814×10^{-3}	1.729814×10^{-3}	4.336809×10^{-19}	/	/
	BBO	2.301350×10^{-3}	6.243230×10^{-3}	1.071160×10^{-2}	1.543310×10^{-3}	>2000	>5.85746
	TLBO	2.141840×10^{-3}	2.610550×10^{-3}	3.329680×10^{-3}	3.125230×10^{-4}	>2000	>5.836608
proposed	BB-TLBO	1.729814×10^{-3}	1.729814×10^{-3}	1.729814×10^{-3}	6.616421×10^{-19}	134	0.169081
2DM							
[57]	SDO	1.729800×10^{-3}	1.811800×10^{-3}	2.028800×10^{-3}	7.242100×10^{-5}	/	/
[55]	ELPSO	1.830700×10^{-3}	2.035100×10^{-3}	2.117800×10^{-3}	8.427100×10^{-5}	/	/
	BBO	3.292930×10^{-3}	5.573130×10^{-3}	9.093230×10^{-3}	1.479270×10^{-3}	>2000	>8.0379308
	TLBO	1.891110×10^{-3}	3.490130×10^{-3}	5.263350×10^{-3}	8.689140×10^{-4}	>2000	>6.3345426
proposed	BB-TLBO	1.693885×10^{-3}	1.694230×10^{-3}	1.697676×10^{-3}	8.587814×10^{-7}	117	5.415939
3DM							
	BBO	3.366020×10^{-3}	4.878470×10^{-3}	5.759890×10^{-3}	5.820820×10^{-4}	>2000	>8.4645975
	TLBO	1.805210×10^{-3}	3.299990×10^{-3}	5.131280×10^{-3}	1.097240×10^{-3}	>2000	>6.3790644
proposed	BB-TLBO	1.689064×10^{-3}	1.689064×10^{-3}	1.707124×10^{-3}	1.294738×10^{-5}	110	6.066541

- It can be seen that BB-TLBO achieved the best results after 134 iterations and 117 iterations for 1DM and 2DM respectively. It features the lowest CPU time (0.169081 s (1DM) and 5.415939 s (2DM)) with the lowest STD value ($STD = 1.64 \times 10^{-15}$ (1DM) and $STD = 9.00 \times 10^{-6}$ (2DM)) and the smallest RMSE value (1.73×10^{-3} (1DM) and 1.69×10^{-3} (2-MD)).
- From the results shown in the table, both BB-TLBO and IQSODE give the same RMSE values in terms of ($RMSE_{min}$, $RMSE_{mean}$ and $RMSE_{max}$). However, in terms of STD the BB-TLBO algorithm obtained the second-best result with a value of 6.616421×10^{-19} following the IQSODE algorithm that obtained a value of 4.336809×10^{-19} .
- For 3DM, the best STD ($STD = 1.294738 \times 10^{-5}$) is obtained by BB-TLBO which reaches the minimum RMSE value of 1.689064×10^{-3} after only 110 iterations in 6.066541s Thus, the proposed BB-TLBO algorithm is stable and reliable to identify the parameters of RTC France silicon solar cell and STM6-40/36 solar module.

4.3. Convergence Analysis

The convergence curves of BB-TLBO and other algorithms such as BBO, TLBO, SCE, SFLA, DE and ABC (when identifying RTC France silicon solar cell and STM6-40/36 solar module for the three models (1DM, 2DM and 3DM)) are shown in Figures 10 and 11.

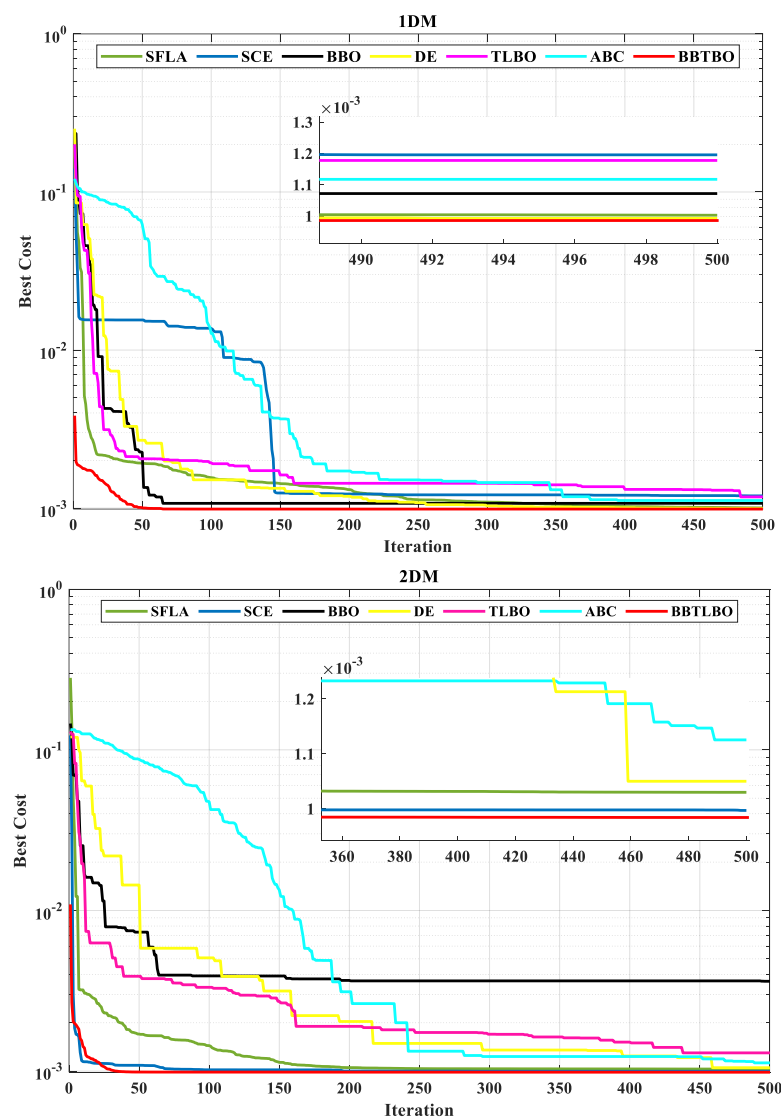


Figure 10. Cont.

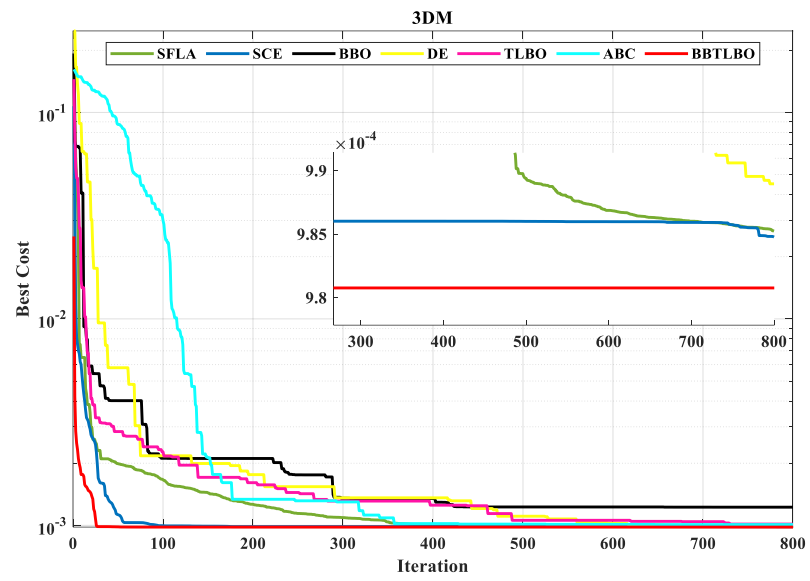


Figure 10. Convergence curves for three models of RTC France silicon solar cell.

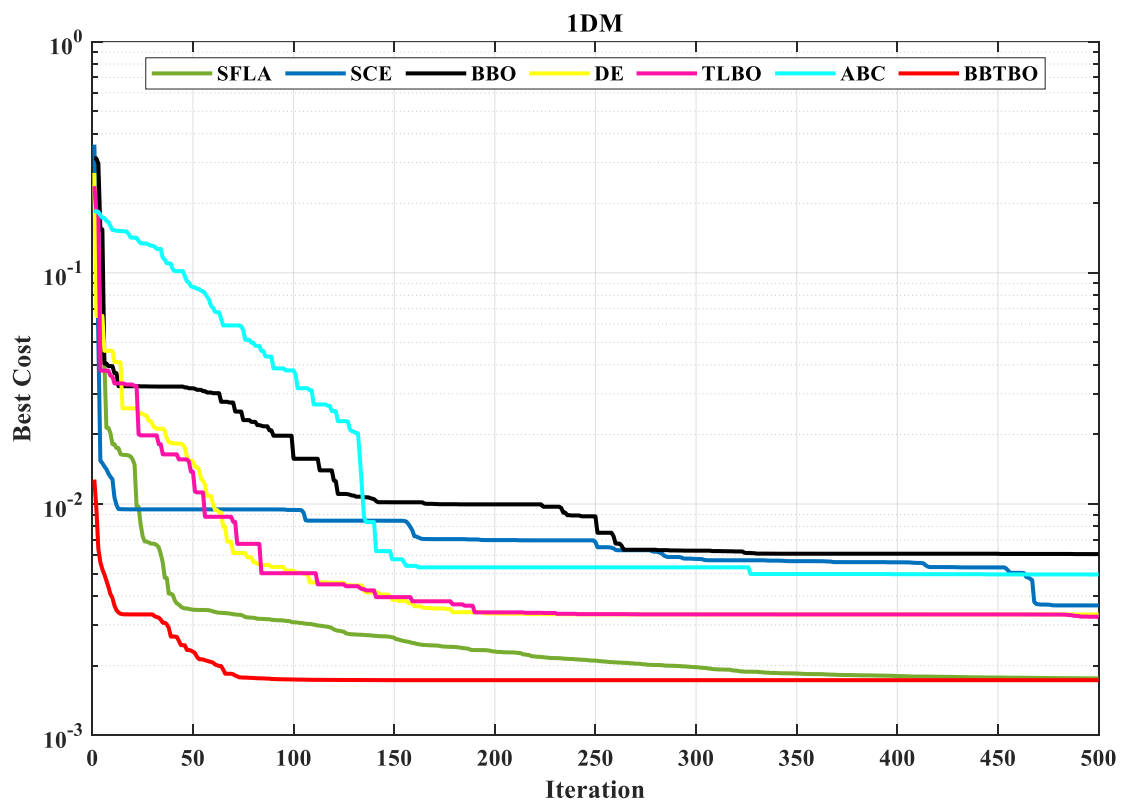


Figure 11. Cont.

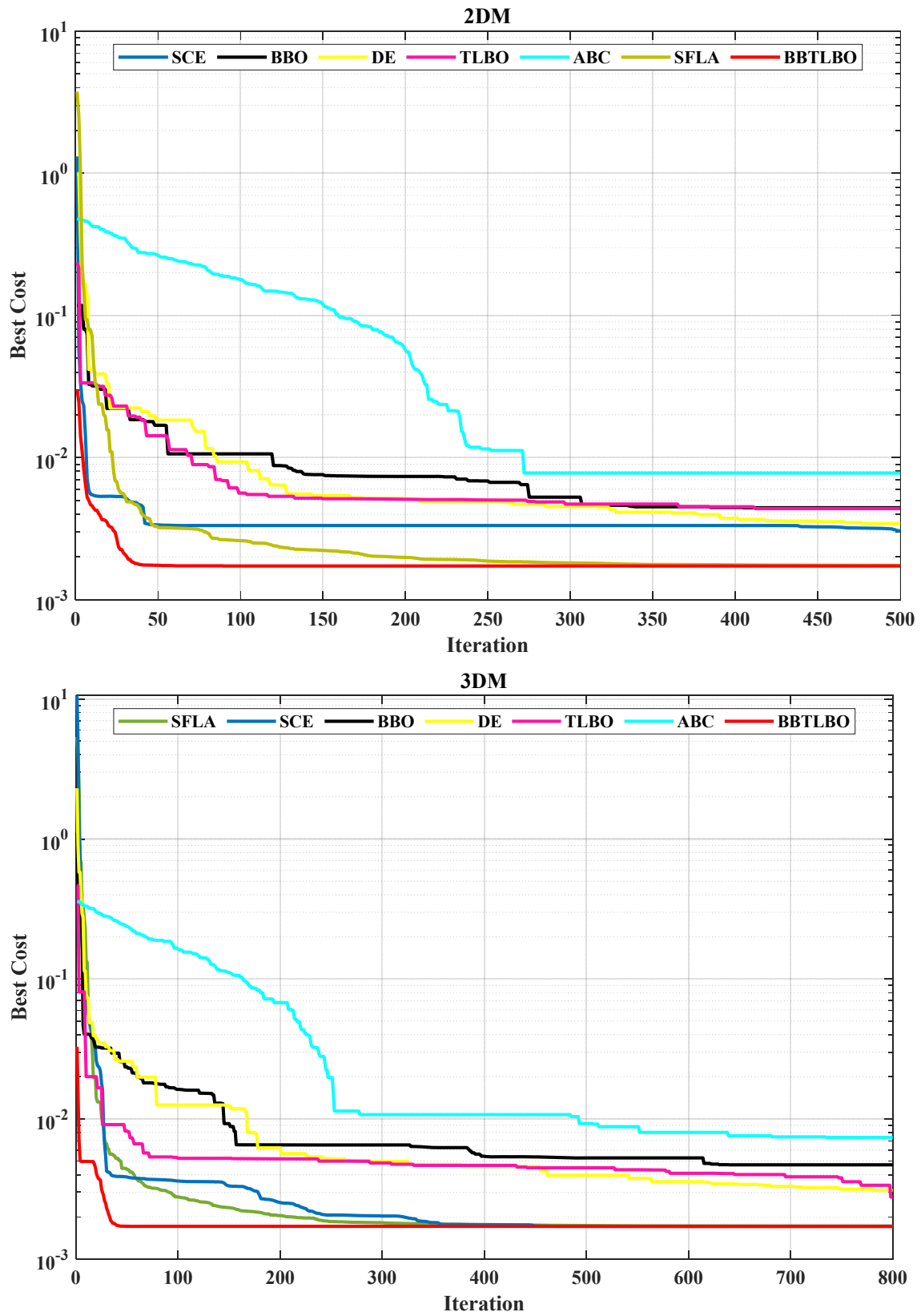


Figure 11. Convergence curves for three models of STM6-40/36 module.

According to these figures, the BB-TLBO algorithm has the best convergence speed compared to the other algorithms in all cases.

5. Conclusions

This article deals with the problem of identifying unknown parameters related to several models of solar cells and modules. Biogeography-based teaching learning-based optimization (BB-TLBO) is suggested as a new optimization algorithm to solve this problem. This algorithm combines two metaheuristic algorithms called: biogeography-based optimization (BBO) and teaching learning-based optimization (TLBO). The root mean square error (RMSE) is used as an objective function. To check the efficiency of BB-TLBO, it is applied to one-diode model (1DM), two-diode model (2DM) and three-diode model (3DM) of silicon solar cell RTC France and commercial PV solar modules, the monocrystalline STM6-40/36.

The following points can be drawn from the results discussed above:

- (i) BB-TLBO performs better in terms of robustness and reliability according to comparison Tables 4 and 5. It revealed the smallest RMSE value in all models of France RTC cell and STM6-40/36 module
- (ii) BB-TLBO has a very high accuracy in terms of the identification of parameters according to IAE, I-V and P-V characteristics.
- (iii) According to the statistical results (RMSE, STD, CPU and It(s) values), BB-TLBO outperforms its own single algorithms (BBO and TLBO) as well as other newly techniques such as DOLADE, IQSODE, IMFOL, ... etc. For example, BB-TLBO records the best statistical results (RMSE = 1.729814×10^{-3} , STD = 6.616421×10^{-19} , CPU = 0.17 s, It(s) = 134) when identifying parameters of STM6-40/36 presented on 1DM, and it records the smallest RMSE in less than 6 s, RMSE = 1.693885×10^{-3} for 2DM and RMSE = 1.689064×10^{-3} for 3DM representations.
- (iv) Convergence curves demonstrated that BB-TLBO has a very fast convergence speed.
- (v) From the results mentioned above, it is clear that the three-diode model (3DM) is the more accurate model to model the RTC France silicon solar cell and the STM6-40/36 solar module.

Overall, The BB-TLBO algorithm is proven to be superior to other recently introduced parameter extraction strategies in terms of precision, stability, and speed through experiments. Consequently, the proposed BB-TLBO can be applied as an effective alternative solution to the issue of PV model parameter extraction.

Author Contributions: Methodology, N.R.; Software, N.R.; Validation, N.R. and K.Y.; Formal analysis, N.R.; Investigation, N.R., A.A., F.H., N.D., B.A.S. and K.Y.; Writing—original draft, N.R.; Writing—review & editing, N.R., A.A., F.H., N.D., B.A.S. and K.Y.; Visualization, N.R., A.A., F.H. and N.D.; Supervision, A.A., F.H. and K.Y.; Funding acquisition, B.A.S. All authors have read and agreed to the published version of the manuscript.

Funding: This research received no external funding.

Data Availability Statement: The data that support the findings of this study are available from the corresponding author upon reasonable request.

Acknowledgments: This work was supported by the General Directorate for Scientific Research and Technological Development (DGRSDT), Algeria.

Conflicts of Interest: The authors declare that they have no known competing financial interest or personal relationships that could have appeared to influence the work reported in this paper.

Appendix A

- For RTC France solar cell

$I_{measured} (A)$	$V_{measured} (V)$
0.764	-0.2057
0.762	-0.1291
0.7605	-0.0588
0.7605	0.0057
0.76	0.0646
0.759	0.1185
0.757	0.1678
0.757	0.2132
0.7555	0.2545
0.754	0.2924
0.7505	0.3269
0.7465	0.3585
0.7385	0.3873
0.728	0.4137
0.7065	0.4373
0.6755	0.459
0.632	0.4784
0.573	0.496
0.499	0.5119
0.413	0.5265
0.3165	0.5398
0.212	0.5521
0.1035	0.5633
-0.01	0.5736
-0.123	0.5833
-0.21	0.59

- For STM6-40/36 module

$I_{measured} (A)$	$V_{measured} (V)$
1.663	0
1.663	0.118
1.661	2.237
1.653	5.434
1.65	7.26
1.645	9.68
1.64	11.59
1.636	12.6
1.629	13.37
1.619	14.09
1.597	14.88
1.581	15.59
1.542	16.4
1.524	16.71
1.5	16.98
1.485	17.13
1.465	17.32
1.388	17.91
1.118	19.08
0	21.02

References

1. Jordehi, A.R. Parameter estimation of solar photovoltaic (PV) cells: A review. *Renew. Sustain. Energy Rev.* **2016**, *61*, 354–371. [[CrossRef](#)]
2. Li, S.; Gong, W.; Wang, L.; Yan, X.; Hu, C. A hybrid adaptive teaching–learning-based optimization and differential evolution for parameter identification of photovoltaic models. *Energy Convers. Manag.* **2020**, *225*, 113474. [[CrossRef](#)]
3. Chen, X.; Yu, K.; Du, W.; Zhao, W.; Liu, G. Parameters identification of solar cell models using generalized oppositional teaching learning based optimization. *Energy* **2016**, *99*, 170–180. [[CrossRef](#)]
4. Ogliairi, E.; Dolara, A.; Manzolini, G.; Leva, S. Physical and hybrid methods comparison for the day ahead PV output power forecast. *Renew. Energy* **2017**, *113*, 11–21. [[CrossRef](#)]
5. Orioli, A.; Di Gangi, A. A procedure to calculate the five-parameter model of crystalline silicon photovoltaic modules on the basis of the tabular performance data. *Appl. Energy* **2013**, *102*, 1160–1177. [[CrossRef](#)]
6. Yang, B.; Wang, J.; Zhang, X.; Yu, T.; Yao, W.; Shu, H.; Zeng, F.; Sun, L. Comprehensive overview of meta-heuristic algorithm applications on PV cell parameter identification. *Energy Convers. Manag.* **2020**, *208*, 112595. [[CrossRef](#)]
7. Li, G.; Li, G.; Zhou, M. Model and application of renewable energy accommodation capacity calculation considering utilization level of inter-provincial tie-line. *Prot. Control. Mod. Power Syst.* **2019**, *4*, 1–12. [[CrossRef](#)]
8. Humada, A.M.; Hojabri, M.; Mekhilef, S.; Hamada, H.M. Solar cell parameters extraction based on single and double-diode models: A review. *Renew. Sustain. Energy Rev.* **2016**, *56*, 494–509. [[CrossRef](#)]
9. Abbassi, A.; Gammoudi, R.; Ali Dami, M.; Hasnaoui, O.; Jemli, M. An improved single-diode model parameters extraction at different operating conditions with a view to modeling a photovoltaic generator: A comparative study. *Sol. Energy* **2017**, *155*, 478–489. [[CrossRef](#)]
10. Abbassi, R.; Abbassi, A.; Jemli, M.; Chebbi, S. Identification of unknown parameters of solar cell models: A comprehensive overview of available approaches. *Renew. Sustain. Energy Rev.* **2018**, *90*, 453–474. [[CrossRef](#)]
11. Khanna, V.; Das, B.K.; Bisht, D.; Singh, P.K. A three diode model for industrial solar cells and estimation of solar cell parameters using PSO algorithm. *Renew. Energy* **2015**, *78*, 105–113. [[CrossRef](#)]
12. Allam, D.; Yousri, D.A.; Eteiba, M.B. Parameters extraction of the three diode model for the multi-crystalline solar cell/module using Moth-Flame Optimization Algorithm. *Energy Convers. Manag.* **2016**, *123*, 535–548. [[CrossRef](#)]
13. Muci, J.; Conde, A.O.; Sánchez, F.G. New method to extract the model parameters of solar cells from the explicit analytic solutions of their illuminated I–V characteristics. *Sol. Energy Mater. Sol. Cells* **2006**, *90*, 352–361. [[CrossRef](#)]
14. Gao, X.; Cui, Y.; Hu, J.; Xu, G.; Wang, Z.; Qu, J.; Wang, H. Parameter extraction of solar cell models using improved shuffling complex evolution algorithm. *Energy Convers. Manag.* **2018**, *157*, 460–479. [[CrossRef](#)]
15. Laudani, A.; Fulginei, F.R.; Salvini, A. High performing extraction procedure for the one-diode model of a photovoltaic panel from experimental I–V curves by using reduced forms. *Sol. Energy* **2014**, *103*, 316–326. [[CrossRef](#)]
16. Hejri, M.; Mokhtari, H.; Azizian, M.R.; Ghandhari, M.; Söder, L. On the Parameter Extraction of a Five-Parameter Double-Diode Model of Photovoltaic Cells and Modules. *IEEE J. Photovolt.* **2014**, *4*, 915–923. [[CrossRef](#)]
17. Bendib, T.; Djeflal, F. *Fuzzy-Logic Based Computation for Parameters Identification of Solar Cell Models BT—Transactions on Engineering Technologies*; Yang, G.-C., Ao, S.-I., Gelman, L., Eds.; Springer: Dordrecht, The Netherlands, 2014; pp. 327–338.
18. Almonacid, F.; Rus, C.; Hontoria, L.; Fuentes, M.; Nofuentes, G. Characterisation of Si-crystalline PV modules by artificial neural networks. *Renew. Energy* **2009**, *34*, 941–949. [[CrossRef](#)]
19. Almonacid, F.; Rus, C.; Hontoria, L.; Muñoz, F.J. Characterisation of PV CIS module by artificial neural networks. A comparative study with other methods. *Renew. Energy* **2010**, *35*, 973–980. [[CrossRef](#)]
20. Pitalúa-Díaz, N.; Arellano-Valmaña, F.; Ruz-Hernandez, J.A.; Matsumoto, Y.; Alazki, H.; Herrera-López, E.J.; Hinojosa-Palafox, J.F.; García-Juárez, A.; Pérez-Enciso, R.A.; Velázquez-Contreras, E.F. An ANFIS-based modeling comparison study for photovoltaic power at different geographical places in Mexico. *Energies* **2019**, *12*, 2662. [[CrossRef](#)]
21. Yousri, D.; Thanikanti, S.B.; Allam, D.; Ramachandaramurthy, V.K.; Eteiba, M.B. Fractional chaotic ensemble particle swarm optimizer for identifying the single, double, and three diode photovoltaic models’ parameters. *Energy* **2020**, *195*, 116979. [[CrossRef](#)]
22. Jordehi, A.R. Time varying acceleration coefficients particle swarm optimisation (TVACPSO): A new optimisation algorithm for estimating parameters of PV cells and modules. *Energy Convers. Manag.* **2016**, *129*, 262–274. [[CrossRef](#)]
23. Pillai, D.S.; Rajasekar, N. Metaheuristic algorithms for PV parameter identification: A comprehensive review with an application to threshold setting for fault detection in PV systems. *Renew. Sustain. Energy Rev.* **2018**, *82*, 3503–3525. [[CrossRef](#)]
24. Ismail, M.S.; Moghavvemi, M.; Mahlia, T.M.I. Characterization of PV panel and global optimization of its model parameters using genetic algorithm. *Energy Convers. Manag.* **2013**, *73*, 10–25. [[CrossRef](#)]
25. Dizqah, A.M.; Maheri, A.; Busawon, K. An accurate method for the PV model identification based on a genetic algorithm and the interior-point method. *Renew. Energy* **2014**, *72*, 212–222. [[CrossRef](#)]
26. Hamid, N.; Abounacer, R.; Idali Oumhand, M.; Feddaoui, M.; Agliz, D. Parameters identification of photovoltaic solar cells and module using the genetic algorithm with convex combination crossover. *Int. J. Ambient. Energy* **2019**, *40*, 517–524. [[CrossRef](#)]
27. Liao, Z.; Gu, Q.; Li, S.; Hu, Z.; Ning, B.I.N. An improved differential evolution to extract photovoltaic cell parameters. *IEEE Access* **2020**, *8*, 177838–177850. [[CrossRef](#)]

28. Chellaswamy, C.; Ramesh, R. Parameter extraction of solar cell models based on adaptive differential evolution algorithm. *Renew. Energy* **2016**, *97*, 823–837. [[CrossRef](#)]
29. Zhou, J.; Zhang, Y.; Zhang, Y.; Shang, W.; Yang, Z. Parameters identification of photovoltaic models using a differential evolution algorithm based on elite and obsolete dynamic learning. *Appl. Energy* **2022**, *314*, 118877. [[CrossRef](#)]
30. Simon, D. Biogeography-Based Optimization. *IEEE Trans. Evol. Comput.* **2008**, *12*, 702–713. [[CrossRef](#)]
31. Niu, Q.; Zhang, L.; Li, K. A biogeography-based optimization algorithm with mutation strategies for model parameter estimation of solar and fuel cells. *Energy Convers. Manag.* **2014**, *86*, 1173–1185. [[CrossRef](#)]
32. Chen, X.; Yu, K. Hybridizing cuckoo search algorithm with biogeography-based optimization for estimating photovoltaic model parameters. *Sol. Energy* **2019**, *180*, 192–206. [[CrossRef](#)]
33. Niccolai, A.; Dolara, A.; Ogliari, E. Hybrid PV Power Forecasting Methods: A Comparison of Different Approaches. *Energies* **2021**, *14*, 451. [[CrossRef](#)]
34. Louzazni, M.; Craciunescu, A.; Aroudam, E.H.; Dumitrache, A. Identification of Solar Cell Parameters with Firefly Algorithm. In Proceedings of the 2015 Second International Conference on Mathematics and Computers in Sciences and in Industry (MCSI), Sliema, Malta, 17 August 2015; pp. 7–12. [[CrossRef](#)]
35. Sudhakar Babu, T.; Prasanth Ram, J.; Sangeetha, K.; Laudani, A.; Rajasekar, N. Parameter extraction of two diode solar PV model using Fireworks algorithm. *Sol. Energy* **2016**, *140*, 265–276. [[CrossRef](#)]
36. Olabi, A.G.; Rezk, H.; Abdelkareem, M.A.; Awotwe, T.; Maghrabie, H.M.; Selim, F.F.; Rahman, S.M.A.; Shah, S.K.; Zaky, A.A. Optimal Parameter Identification of Perovskite Solar Cells Using Modified Bald Eagle Search Optimization Algorithm. *Energies* **2023**, *16*, 471. [[CrossRef](#)]
37. Shaheen, A.M.; El-Seheimy, R.A.; Xiong, G.; Elattar, E.; Ginidi, A.R. Parameter identification of solar photovoltaic cell and module models via supply demand optimizer. *Ain Shams Eng. J.* **2022**, *13*, 101705. [[CrossRef](#)]
38. El-Dabah, M.A.; El-Sehiemy, R.A.; Hasanien, H.M.; Saad, B. Photovoltaic model parameters identification using Northern Goshawk Optimization algorithm. *Energy* **2023**, *262*, 125522. [[CrossRef](#)]
39. Gao, X.; Cui, Y.; Hu, J.; Xu, G.; Yu, Y. Lambert W-function based exact representation for double diode model of solar cells: Comparison on fitness and parameter extraction. *Energy Convers. Manag.* **2016**, *127*, 443–460. [[CrossRef](#)]
40. Ginidi, A.R.; Shaheen, A.M.; El-sehiemy, R.A.; Elattar, E. Supply demand optimization algorithm for parameter extraction of various solar cell models. *Energy Rep.* **2021**, *7*, 5772–5794. [[CrossRef](#)]
41. Yu, K.; Chen, X.; Wang, X.; Wang, Z. Parameters identification of photovoltaic models using self-adaptive teaching-learning-based optimization. *Energy Convers. Manag.* **2017**, *145*, 233–246. [[CrossRef](#)]
42. Rao, R.V.; Savsani, V.J.; Vakharia, D.P. Teaching-Learning-Based Optimization: An optimization method for continuous non-linear large scale problems. *Inf. Sci.* **2012**, *183*, 1–15. [[CrossRef](#)]
43. Chen, X.; Xu, B.; Mei, C.; Ding, Y.; Li, K. Teaching-learning-based artificial bee colony for solar photovoltaic parameter estimation. *Appl. Energy* **2018**, *212*, 1578–1588. [[CrossRef](#)]
44. Li, S.; Gong, W.; Yan, X.; Hu, C.; Bai, D.; Wang, L.; Gao, L. Parameter extraction of photovoltaic models using an improved teaching-learning-based optimization. *Energy Convers. Manag.* **2019**, *186*, 293–305. [[CrossRef](#)]
45. Long, W.; Cai, S.; Jiao, J.; Xu, M.; Wu, T. A new hybrid algorithm based on grey wolf optimizer and cuckoo search for parameter extraction of solar photovoltaic models. *Energy Convers. Manag.* **2020**, *203*, 112243. [[CrossRef](#)]
46. Naeijian, M.; Rahimnejad, A.; Ebrahimi, S.M. Parameter estimation of PV solar cells and modules using Whippy Harris Hawks Optimization Algorithm. *Energy Rep.* **2021**, *7*, 4047–4063. [[CrossRef](#)]
47. Xavier, F.J.; Pradeep, A.; Premkumar, M.; Kumar, C. Orthogonal learning-based Gray Wolf Optimizer for identifying the uncertain parameters of various photovoltaic models. *Optik* **2021**, *247*, 167973. [[CrossRef](#)]
48. Kumar, C.; Raj, T.D.; Premkumar, M.; Raj, T.D. A new stochastic slime mould optimization algorithm for the estimation of solar photovoltaic cell parameters. *Optik* **2020**, *223*, 165277. [[CrossRef](#)]
49. Qaraad, M.; Amjad, S.; Hussein, N.K.; Badawy, M.; Mirjalili, S.; Elhosseini, M.A. Photovoltaic parameter estimation using improved moth flame algorithms with local escape operators. *Comput. Electr. Eng.* **2023**, *106*, 108603. [[CrossRef](#)]
50. Yu, S.; Heidari, A.A.; He, C.; Cai, Z.; Althobaiti, M.M.; Mansour, R.F.; Liang, G.; Chen, H. Parameter estimation of static solar photovoltaic models using Laplacian Nelder-Mead hunger games search. *Sol. Energy* **2022**, *242*, 79–104. [[CrossRef](#)]
51. Long, W.; Jiao, J.; Liang, X.; Xu, M.; Tang, M.; Cai, S. Parameters estimation of photovoltaic models using a novel hybrid seagull optimization algorithm. *Energy* **2022**, *249*, 123760. [[CrossRef](#)]
52. El-mageed, A.A.A.; Abohany, A.A.; Saad, H.M.H.; Sallam, K.M. Parameter extraction of solar photovoltaic models using queuing search optimization and differential evolution. *Appl. Soft Comput.* **2023**, *134*, 110032. [[CrossRef](#)]
53. Shaban, H.; Houssein, E.H.; Pérez-cisneros, M.; Oliva, D.; Hassan, A.Y.; Ismaeel, A.A.K.; Abdelminaam, D.S.; Deb, S.; Said, M. Identification of Parameters in Photovoltaic Models through a Runge Kutta Optimizer. *Mathematics* **2021**, *9*, 2313. [[CrossRef](#)]
54. Li, Y.; Yu, K.; Liang, J.; Yue, C.; Qiao, K. A landscape-aware particle swarm optimization for parameter identification of photovoltaic models. *Appl. Soft Comput.* **2022**, *131*, 109793. [[CrossRef](#)]
55. Jordehi, A.R. Enhanced leader particle swarm optimisation (ELPSO): An efficient algorithm for parameter estimation of photovoltaic (PV) cells and modules. *Sol. Energy* **2018**, *159*, 78–87. [[CrossRef](#)]
56. Xiong, G.; Zhang, J.; Shi, D.; Zhu, L.; Yuan, X.; Yao, G. Modified Search Strategies Assisted Crossover Whale Optimization Algorithm with Selection Operator for Parameter Extraction of Solar Photovoltaic Models. *Remote Sens.* **2019**, *11*, 2795. [[CrossRef](#)]

57. Xiong, G.; Zhang, J.; Shi, D.; Yuan, X. Application of Supply-Demand-Based Optimization for Parameter Extraction of Solar Photovoltaic Models. *Complexity* **2019**, *2019*, 3923691. [[CrossRef](#)]
58. Premkumar, M.; Babu, T.S.; Umashankar, S.; Sowmya, R. A new metaphor-less algorithms for the photovoltaic cell parameter estimation. *Optik* **2020**, *208*, 164559. [[CrossRef](#)]
59. Yu, K.; Liang, J.J.; Qu, B.Y.; Cheng, Z.; Wang, H. Multiple learning backtracking search algorithm for estimating parameters of photovoltaic models. *Appl. Energy* **2018**, *226*, 408–422. [[CrossRef](#)]

Disclaimer/Publisher's Note: The statements, opinions and data contained in all publications are solely those of the individual author(s) and contributor(s) and not of MDPI and/or the editor(s). MDPI and/or the editor(s) disclaim responsibility for any injury to people or property resulting from any ideas, methods, instructions or products referred to in the content.